A SOFTWARE DEFINED RADIO EXPERIMENTAL PLATFORM FOR GPS/GNSS SIGNAL RECEPTION ANALYSIS

A Thesis

by

LINGJUN PU

Submitted to the Office of Graduate and Professional Studies of
Texas A&M University
in partial fulfillment of the requirements for the degree of

MASTER OF SCIENCE

Chair of Committee,	Jyh-Charn (Steve) Liu
Co-Chair of Committee,	Gwan Choi
Committee Member,	Srinivas Shakkottai
Head of Department,	Miroslav Begovic

August 2015

Major Subject: Computer Engineering

ABSTRACT

GPS is becoming a crucial element in daily life and in global information infrastructure. GPS nowadays is becoming more reliable thanks to the technology of A-GPS and D-GPS which uses the Internet and cellular network to enhance the accuracy. However, there is still plenty of room for improvement in the GPS operations. A versatile experimental platform that allows researchers to directly receive raw data from satellites is critical to advance further research.

We use a software defined radio (USRP) platform with open source GNSS software to perform the related experiments. We choose the USRP N200 as the software defined radio (SDR) for our work, because of its very good signal processing performance at an affordable price. Unlike mobile phones, or even most GPS chip evaluation kits. The GPS data received from USRP can be utilized to compute pseudo ranges based different satellites. And the pseudo range can be valuable when analyzing the accuracy of computing the locations. With the open source software, the users can easily access and customize their own software development to target the specific application.

We built a portable experimental environment based the USRP to carry out field tests at various locations. Two additional limitations of GPS chip evaluation kits are their low quality clocks, and very limited computing resources for more sophisticated experiments.

This thesis will talk about this portable software platform and the project which was conducted on it to explore and investigate some crucial problems existing in today's GNSS technology, for example, multipath problem and hybrid GNSS system problem.

By investigating into these problems using SDR GNSS receiver, the benefits of adopting this software oriented approach will be talked about and how this approach in the future can save valuable research and experiment time will also be demonstrated.

DEDICATION

To my parents

To my grand parents

ACKNOWLEDGEMENTS

I feel really appreciated that my committee co-chair, Dr. Liu, Dr. Choi and my committee member, Dr. Shakkottai provided me with the necessary support to conduct my GNSS research at Texas A&M University.

I would especially thank Dr Liu, who spent his valuable time to read and revise my paper work and provide valuable resources for me to complete the project. Also, I would like to thank my lab partner, Guoyu (Michael) Fu, who worked with me on the GPS experiment and came up with marvelous ideas to solve all kinds of problems. I admire his dedication and passion for GNSS research.

Thanks also go to my friends and lab mates and the department of computer science and engineering and department of electrical and computer engineering for helping me through my research.

Finally, thanks goes to my parents for their support and guidance through my graduate and undergraduate school.

NOMENCLATURE

ASIC	application-specific integrated circuit
GPS	Global Positioning System
B/CS	Bryan/College Station
USRP	Universal Software Radio Peripheral
FPGA	Field-programmable gate array
UHD	Universal Hardware Drive
T	Time
DOT	Texas Department of Transportation
SDR	Software Defined Radio
RF	Radio Frequency
RINEX	Receiver Independent Exchange Format
KML	Keyhole Markup Language
PVT	Position, Velocity, Time
NEMA	National Marine Electronics Association
TOA	Time of Arrival
DOP	Dilution of precision
EN	East and North
SNR	Signal to Noise Ratio
ADC	Analog to Digital Converter

TABLE OF CONTENTS

Page

LIST OF FIGURES

Page

LIST OF TABLES

Page

CHAPTER I

INTRODUCTION AND MOTIVATION

I.1 Introduction

Satellite based positioning services has gradually become popular and crucial in all kinds of applications. From transportation in sea, sky and ground to the positioning based mobile applications, it plays a big role by providing the instant location information which can assist the user to access the location based service [2].

Throughout the history, a long time ago, humans already developed navigation technology to explore the world. In ancient China, compass was used to guide the ships in transportation under severe weather conditions.

But Navigation satellite was first designed until early 70s. Three satellites systems were developed before GPS, Transit and Timation from US Navy and 621B plan from the Air Force. At the beginning, this technology was only deployed for military use due to security issues [1].

Until December 1973, GPS project was eventually approved. The first satellite for GPS was launched in 1978 [1]. 15 years later, in August 1993, there were 24 satellites available in the sky. Same year in December, the GPS system became functional for basic operations. The GPS system has a rather short history from first launching to basic

functioning, but it is now available from civilian use to military use and its accuracy has been gradually improved thanks to the newly developed technology [1]. The ability of which, the Global Navigation Satellite System (GNSS) receiver can obtain the three-dimensional location is the major achievement of the last 30 years. Furthermore, the ability of GNSS services, which can provide an accurate time references using its atomic clock, can help the synchronization of distributed computing, for example, ATM transactions, global communications and smart grids [2].

As our world is becoming mobile, and embedded devices such as mobile phones, smart watches can provide us with the services based on the location information from its GNSS receiver, of which, the more accurate the internal receiver can achieve, the better service the application can provide for the users. It is important that the GNSS receiver can guarantee the positioning and timing and can be conscious of the factors which can affect the performance of calculating the position.

In this thesis, we address this issue by proposing a research platform which is based on open source software and dedicated hardware system. The experiments conducted will be discussed and the results will be evaluated to demonstrate the performance of this research platform and how this platform can benefit the GNSS research and community.

I.2 Why do we need an SDR experimental system?

This thesis mainly concerns about the signal quality received from the satellites and finding out the factors which may contribute to the accuracy and precision of calculating the positions. By utilizing the powerful GNSS-SDR, many real time navigation data can be collected and documented for the specific research use. For example, with the help of this research platform, the outdoor field tests can be carried out easily, the data received can be saved and plotted using external analytic software. Some GNSS research can use the recorded data as the validation for certain algorithms developed. Furthermore, the signal processing part can be reconfigured and designed using the software to find out the quality of analog to digital converter, phase lock loop and filters, etc.

The GNSS research has always been a research topic involving with aerospace engineering, geology, electrical engineering and computer science, etc. This mixture of different subjects can be either a big challenge or the chance of collaborating. The goal of this research project is to contribute to the GNSS related research and provide a valuable tool for those researchers to easily acquire the navigation data [20].

The objective of the project is to use the software platform to investigate into GNSS signal receiving problems and analyze the performance by utilizing different receiving configurations so that the users in the future can use this research as a reference to

design customized receiver. The data gathered from the research will be saved for future use.

Software defined radio system we used in the experiments is USRP N200, which can provide a high-bandwidth, high dynamic range processing capability. It features a Xilinx Spartan 3A-DSP 1800 FPGA, 100MS/s dual ADC, 400MS/s dual DAC and Gigabit Ethernet connectivity which can streams large GNSS receiving data to be processed on host PC [4].

The maximum stream data rate to the host PC can be up to 50MS/s. FPGA board can be reprogrammed to meet the customer needs. The UHD driver already provides the user with the ability to erase or upload the latest firmware.

The technical details of USRP N200 are listed in Table 1-1:

USRP N200 Specifications	Typical	Unit
ADC Sample Rate	100	MS/s
ADC Resolution	14	bits
ADC Wideband SFDR	88	dBc
DAC Sample Rate	400	MS/s
DAC Resolution	16	bits
DAC Wideband SFDR	80	dBc
Host Sample Rate (8b/16b)	50/25	MS/s
Frequency Accuracy	2.5	ppm
with GPSDO Reference	0.01	ppm

Table 1-1 USRP N200 specification [4]

N200 also can work together with all kinds of software like LabVIEW, GNU Radio, or even Simulink.

Although GNSS simulation software is often accepted as the alternative way to conduct real-time GNSS signal processing experiment. They can't represent the complexity of real-time live sky signal. The real world signal usually makes up of the signals reflected from the rooftop or walls of the building and these scenarios couldn't be modelled perfectly just using simulator [5].

Another problem of using GNSS signal simulator is that the hardware/software system is so dedicated that the cost of modelling the signal can be quite high comparing to only capture the real-time outdoor signals.

So why don't we use an evaluation kit or Microcontroller based hardware system? In Table 1-2 displays the comparison of USRP platform and other platforms:

Comparison	USRP based hardware	SiGe GN3S Sampler	GNSS Simulator
Bandwidth	25 MHz	2 - 4 MHz	16 MHz
Center Frequency	0.8 -2.35 GHz	1575.42 MHz	1575.42 MHz & 1602 MHz
Constellation	GPS/GLONASS/Galileo/Compass	GPS/Galileo	GPS/GLONASS
Sampling Frequency	Complex, up to 25 Msps	Real, up to 16 Msps	complex, 16.368 Msps
Quantization	14 bit	2 bit	2 bit or 4 bit

Table 1-2 GNSS front-ends comparison [6]

From the Table 1-2, USRP platform can have a wider bandwidth and radio frequency coverage different from other RF front-ends [6]. Another important contrast with normal front-ends is that the software utilized GNSS-SDR can record the pseudorange from

satellites and generate the RINEX file format file which can be used as the experimental data for signal spoofing and multipath detection problems. While most other platforms wouldn't provide the user with the pseudorange information [6].

At the beginning stage of the research, we were thinking of using SiGe GN3S Sampler v3 as the platform, but it is already out of stock and the sampling time is only 160s which is quite short for our research to observe the signal to noise ratio of the satellites in urban canyon environment.

Another method of obtaining the RINEX file is through Continuously Operating Reference Station (CORS). "Global Navigation Satellite System (GNSS) data consisting of carrier phase and code range measurements" can be provided [7]. In Bryan/College Station, there is only one CORS – TXBX in Figure 1-1, which can sample the data every 5 seconds [7]. The location of the CORS is static and it has the non-blocking skyview of satellites which somehow limit the research scope of exploring the effects of multipath signal. The CORS station can only capture the GLONASS and GPS data, which also restrict the scope of research of the hybrid GNSS systems.

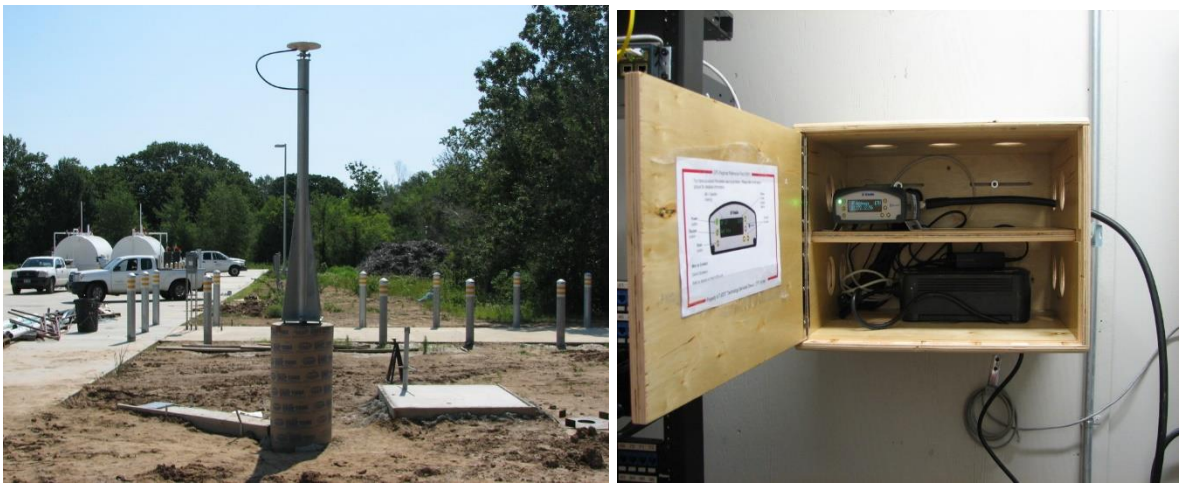

Figure 1-1 CORS station in Bryan [7]

So why not a mobile phone? As it is known, nowadays mobile phones are equipped with dedicated GNSS chip which provides the location based services and applications without knowing what exactly how the GNSS chip can obtain the information from the satellite. For example, the location framework provided by Apple iOS can directly tell the user geographical coordinates as well as the accuracy of the measurement. Same as Android devices whose Java package contains the functions to get the user coordinates [2]. To conclude, mobile phones just provide the coding instructions for the users which can abstractly obtain the information necessary of the service. But the user has no idea about which satellite's data can be observed or has the ability to modify the internal receiver configurations. Furthermore, with the development of new GNSS systems, the receiver designer needs the opportunity to modify the existing receiver and design the new receiver based on that [2].

From the comparison with various GNSS receivers, it is necessary for the receiver designers to adapt software defined radio paradigm. The RF front-end, such as USRP, can perform the frequency down conversion before other signal processing procedure, the software itself can deal with the signal and data processing which provides high flexibility for the developers to fully access and modify the whole receiver [2]. The detailed discussion about this flexible software framework is on later this chapter as well as chapter 3.

I.3 Basic principles for GNSS receiver

The procedure for the GNSS receiver of receiving the signal from the satellites is in Figure 1-2. The signals are captured by the front-end antenna, the signal is usually quite small, and is amplified by the analog circuits. The frequency of the signal is down converted to the necessary frequency range [9]. After that, ADC can transform the signal from analog to digital.

The procedure in the last paragraph is the hardware parts of the receiver, then the signal needs processing using the software. As we can see here, the hardware part takes responsibility of preprocessing the signal and is configured to be static. But the software part of the receiver has more flexibilities in configurations. The software can be configured to change the functionality of radio frequency signals, both for the amplitude

or the frequency of the signal. In this project, we gained lots of benefits of using this software approach shown as the computer in Figure 1-2 to save hardware developing and debugging time.

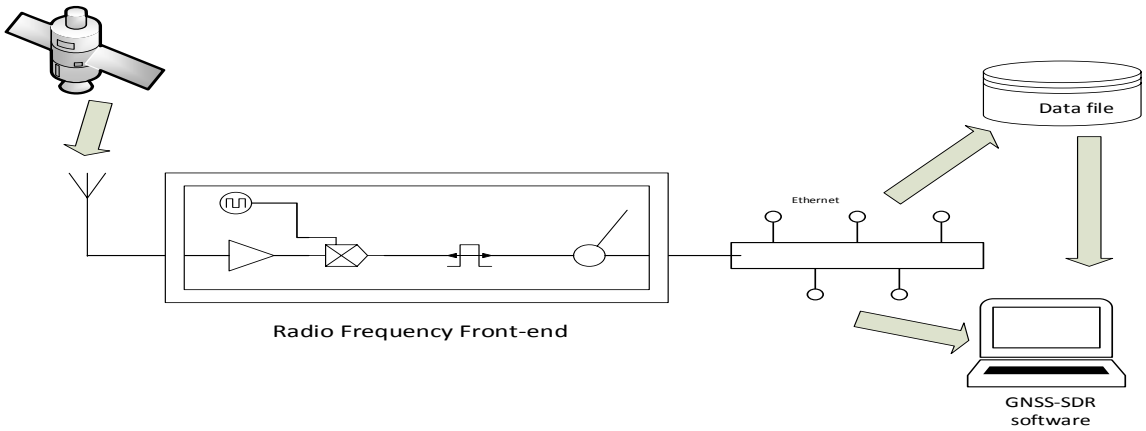

Figure 1-2 Overall hardware/software System [2]

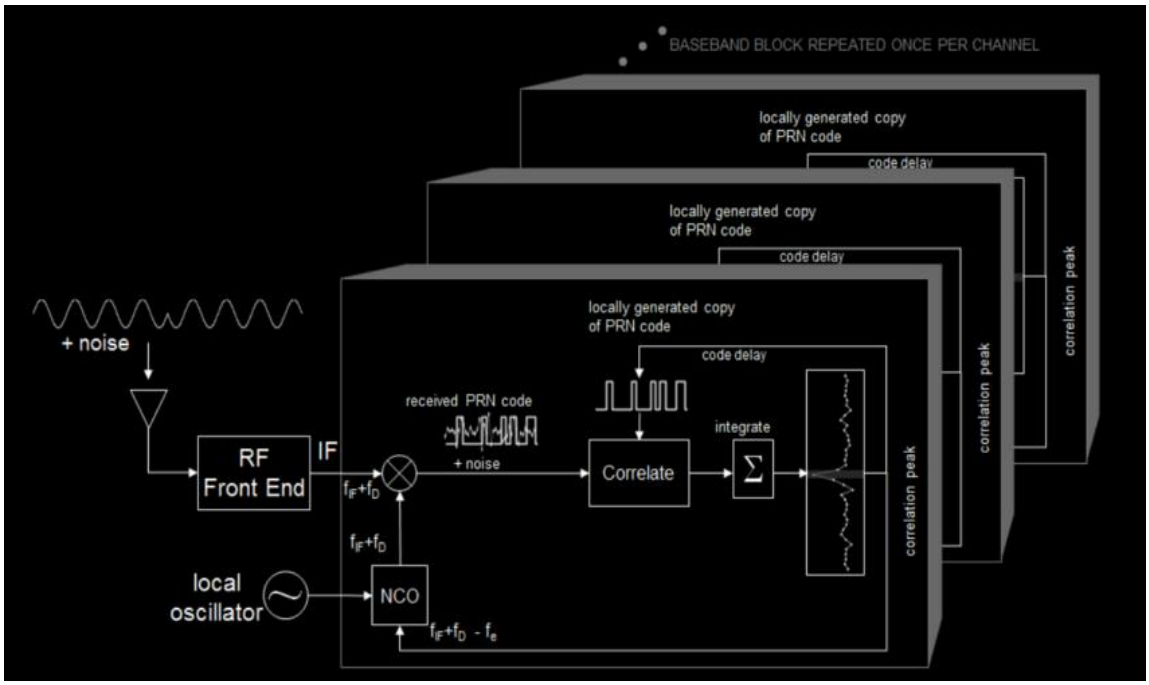

Figure 1-3 Multi-Channel receiver architecture [8]

In the above Figure 1-3 shows the architecture for multi-channel GNSS receiver case.

I.4 Advantages of using software approach

Using software approach can handle the data received from various kinds of hardware system. And different kinds of data can be rewritten and converted to each other depending on the data type received for the specific hardware so that using the software approach provides a flexible way of sampling and processing data.

With the development of new algorithms for tracking satellites and receiving the data. The software can be redesigned to feature the users' need without designing the new hardware system.

In this thesis, we use GNSS-SDR as mentioned before, official website claims that GNSS-SDR "implements a global navigation satellite system software defined receiver" using the C++ programming language [21]. The design of GNSS-SDR architecture allows all kinds of customization and "provides an interface to different" RF front-end receivers [21]. The user can design a GNSS software by defining the dataflow and signal processing methodology to implement in C++ code.

The following diagram Figure 1-4 demonstrates the overall dataflow scheme of the software architecture.

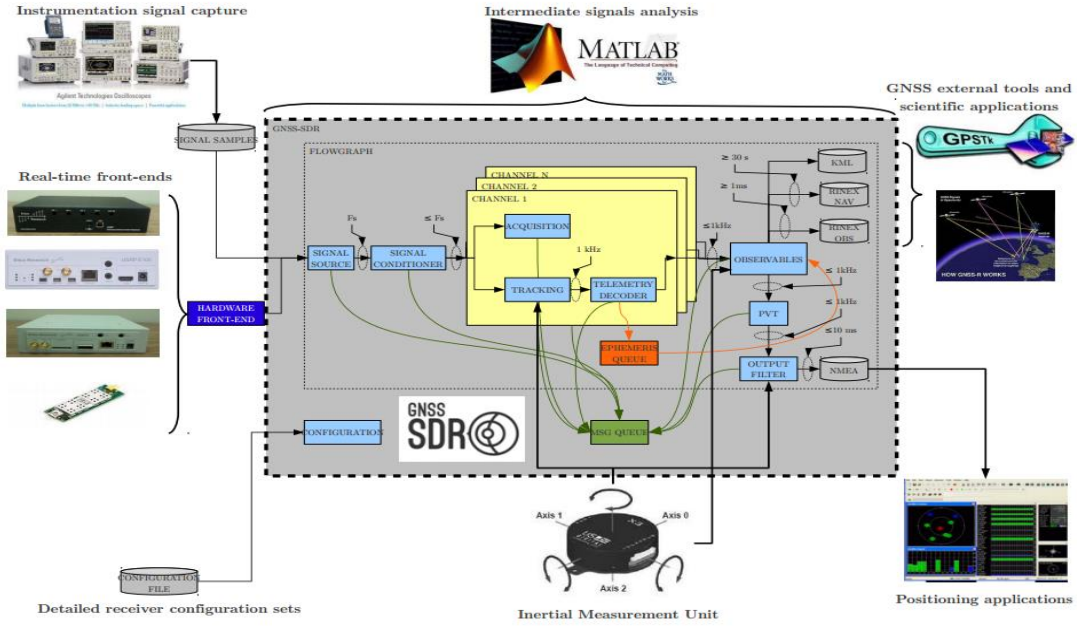

Figure 1-4 Architecture of GNSS-SDR software package [3]

Some additional advantages of using this architecture are:

This software platform can provide the code with high efficiency and high reusability. The documentation contains the description of the framework so that the user can refer to that as the development guidelines.

This platform has also been tested and optimized on various hardware and takes advantages of the multicore processors on the host computers. In addition, from the diagram on the left side, the platform can process the data either in real time mode or post-processing mode [21]. The real-time signal is processed once the signal is coming and the post-processing mode uses the data saved as raw bit files to process.

The software platform can acquire the signal and track the satellites available. It then decodes the navigation messages and saves the necessary information to compute the position. Either the observed data can be saved as RINEX file which contains the pseudorange and users can use external GNSS software to analyze and visualize the data, or the software itself can create a computed position saved in KML file format.

CHAPTER II

BACKGROUND KNOWLEDGE

II.1 Introduction

It is important to understand some concepts of the navigation technology to better design the new algorithms for SDRs. This chapter starts with how the receiver can calculate the position, to the characteristics of the satellite signals (GPS) and how the signal can be processed. As the knowledge base of the GNSS technology is quite large and different navigation systems, such as GPS, Galileo, Beidou, are operated using various technologies. The chapter will mainly focus on the GPS technology and the general operation of the GPS system.

II.2 Concept of Time of Arrival (TOA)

The satellite itself is at the known location and the receiver's location is not yet known. GPS technology utilizes the TOA to calculate the receiver location. From definition, "TOA is the time needed for the signal to travel from the satellite to the receiver" [9].

This time interval, which is also called the propagation time of the satellite signal, can be multiplied by the signal speed, generally speed of light, to obtain the distance from the satellite to the receiver, however this is not quite accurate as there are many unknown propagation contributing factors which can somehow change this distance [9].

II.3 Determine the position

In the following Figure 2-1 is the demonstration of the measurement from the satellite to the receiver. The receiver is located somewhere on the sphere. The satellite is at the center of the sphere.

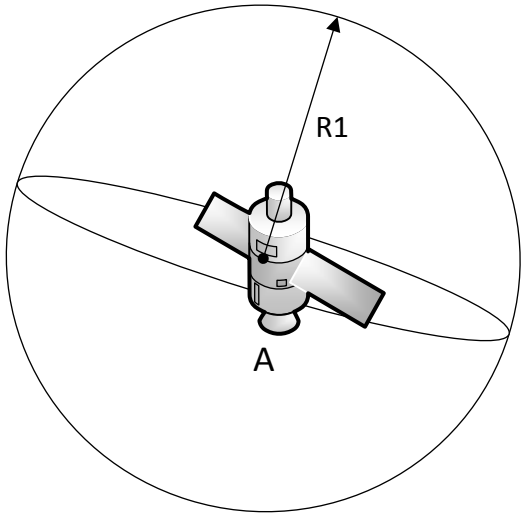

Figure 2-1 One satellite condition

With two satellites on the diagram below, a similar sphere centered at B with the radius $R_{2,}$ also we have the previous sphere centered at A with radius R_1. Under this circumstance, the position of the receiver can be either at the location of the two dots in Figure 2-2.

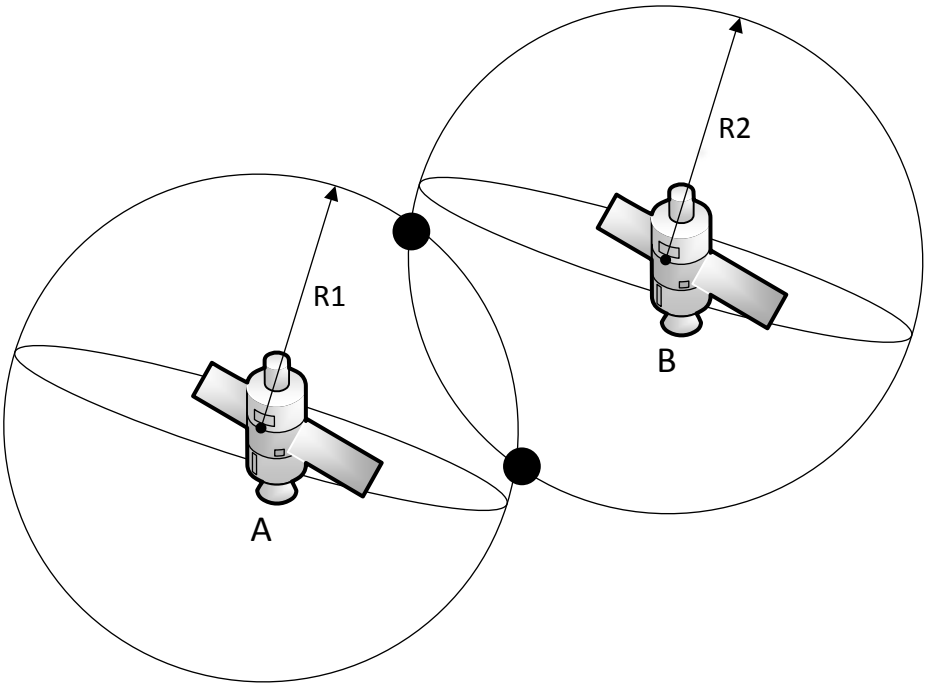

Figure 2-2 Two satellite condition

Adding one more sphere, which is C, with the radius R_3, shown in Figure 2-3 below. The only receiver which is at the intersection of these three spheres is dot on the diagram which is the position of the receiver.

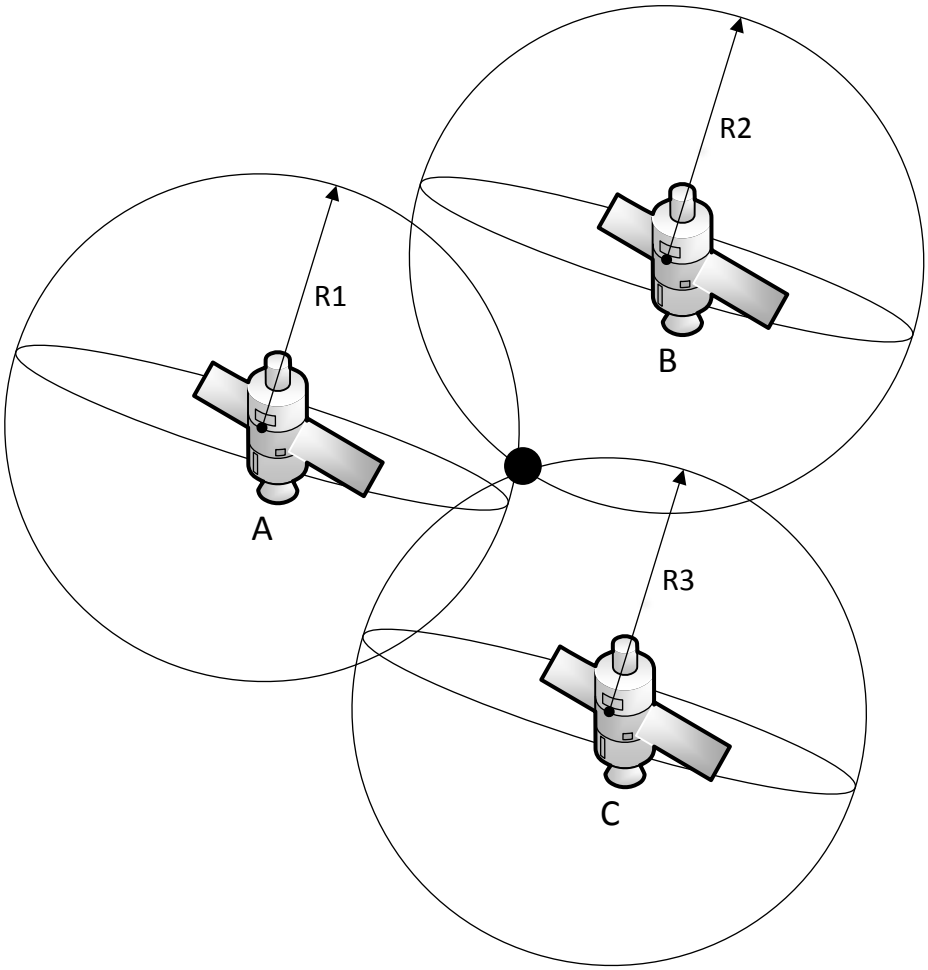

Figure 2-3 Three satellite condition

The three satellites condition can help determine the position of the receiver in a 2 dimensional plane. However, in a 3 dimensional space, we need at least 4 satellites which means 4 measurements of the distance from the satellites to determine the position of the user. This can be demonstrated as the following. Two spheres can intercept each other to obtain a circle. And another sphere can intercept the circle to obtain 2 possible

locations shown as Figure 2-2. Yet another satellite is required to determine the position shown as Figure 2-3.

The three diagrams above assume that the measurement between the satellite and the user is accurate, no errors included. However, in reality, the distance measured between the receiver and satellites contains some unknown discrepancy as the user clock is different from satellite atomic clock [9]. In order to resolve this discrepancy, yet another satellite (5^{th}) is needed [9].

As discussed before, the least satellites required to obtain the user location are just 4.

II.4 Basic functions to determine the user position

Assume that we have three known points r_1 (x_1, y_1, z_1), r_2 (x_2, y_2, z_2), r_3 (x_3, y_3, z_3) and an unknown point r_u (x_u, y_u, z_u) [9]. If the measurement of the distance between the unknown point and 3 known points are already acquired, we can obtain the following three equations [9].

$$\rho_1 = \sqrt{(x_1 - x_u)^2 + (y_1 - y_u)^2 + (z_1 - z_u)^2}$$
$$\rho_2 = \sqrt{(x_2 - x_u)^2 + (y_2 - y_u)^2 + (z_2 - z_u)^2} \qquad (2.1)\ [9]$$
$$\rho_3 = \sqrt{(x_3 - x_u)^2 + (y_3 - y_u)^2 + (z_3 - z_u)^2}$$

The functions can solve the x_u, y_u, z_u.. In theory, as these functions are second order, they may have two solutions. The functions are nonlinear, so they can be linearized to solve the equations.

Once acquired, these functions can be used to solve for the user location. As when GPS is working, each satellite can send the signal simultaneously with its own information tags and the receiver need to acquire these signals in a certain time frame to calculate the position.

Assume that a satellite sends the signal at t_1, and the receiver receives the signal later at t_2. The certain satellite i have a distance with the user as

$$\rho_i = c(t_2 - t_1) \qquad (2.2)$$

In this equation, the distance is calculated by multiply the speed of light with the time difference between the receiver and satellite [9].

In reality, obtaining the exact psudeorange is difficult. The actual satellite sending signal time t'_1 and receiver receiving time t'_2 have the relationship as the following [9],

$$t'_1 = t_1 + \Delta b_i$$

$$t'_2 = t_2 + b_u \qquad (2.3)$$

In 2.3, Δb_i is the clock discrepancy of the satellite and b_u is the user clock discrepancy. Not only the clock can contribute to the measurement of the pseudorange, but also

several other factors can influence the measurement accuracy, the overall equation can be expressed as [9]:

$$\rho_i' = \rho_i + \Delta D_i - c(\Delta b_i - b_u) + c(\Delta T_i + \Delta I_i + v_i + \Delta v_i) \quad (2.4)\ [9]$$

In 2.4, ΔD_i is the factor of the discrepancy of the satellite position, ΔT_i, ΔI_i is error caused by troposphere and ionosphere delaying, v_i is the noise error inside the receiver and Δv_i is the timing correction due to the theory of relativity [9].

Some discrepancy can be solved using a dual frequency receiver such as troposphere and ionosphere errors. But the error caused by the user clock is not solvable using the information received from the satellite. It is still an unknown in the equations, so the functions in 2.1 need to be revised as the following [9]:

$$\rho_1 = \sqrt{(x_1 - x_u)^2 + (y_1 - y_u)^2 + (z_1 - z_u)^2} + b_u$$

$$\rho_2 = \sqrt{(x_2 - x_u)^2 + (y_2 - y_u)^2 + (z_2 - z_u)^2} + b_u$$

$$\rho_3 = \sqrt{(x_3 - x_u)^2 + (y_3 - y_u)^2 + (z_3 - z_u)^2} + b_u$$

$$\rho_4 = \sqrt{(x_4 - x_u)^2 + (y_4 - y_u)^2 + (z_4 - z_u)^2} + b_u \quad (2.5)\ [9]$$

In such equation, we have 4 functions for 4 unknown x_u, y_u, z_u and b_u, if the functions are linear, we can obtain the values of 4 unknowns. But in 2.5, the functions are nonlinear, if we still wish to obtain the solutions these functions need to be linearized.

According to the functions listed for 2.5, it is hard to find out the 4 unknown as the functions are not linear. To solve this problem, the functions need to be linearized. The listed function can be transformed to:

$$\rho_i = \sqrt{(x_i - x_u)^2 + (y_i - y_u)^2 + (z_i - z_u)^2} + b_u \qquad (2.6)\ [9]$$

We can differentiate the function above and get the result as:

$$\delta\rho_i = \frac{(x_i - x_u)\delta x_u + (y_i - y_u)\delta y_u + (z_i - z_u)\delta z_u}{\sqrt{(x_i - x_u)^2 + (y_i - y_u)^2 + (z_i - z_u)^2}} + \delta b_u$$

$$= \frac{(x_i - x_u)\delta x_u + (y_i - y_u)\delta y_u + (z_i - z_u)\delta z_u}{\rho_i - b_u} + \delta b_u$$

(2.7) [9]

δx_u, δy_u, δz_u, δb_u are the unknowns in the equation. We can assign the initial values for x_u, y_u, z_u, b_u to just find out the values for the new unknowns in 2.7 [9]. Using new solutions for δx_u, δy_u, δz_u, δb_u, we can modify the original x_u, y_u, z_u, b_u values iteratively [9]. Repeat the above modifications, the values of δx_u, δy_u, δz_u, δb_u can be limited to preliminary thresholds [9]. Then the new values for x_u, y_u, z_u, b_u can be utilized as the final solution for the function [9].

When δx_u, δy_u, δz_u, δb_u are unknowns, the equation of (2.7) becomes linear functions. And the function can be expressed in matrix [9]:

$$\begin{bmatrix} \delta\rho_1 \\ \delta\rho_2 \\ \delta\rho_3 \\ \delta\rho_4 \end{bmatrix} = \begin{bmatrix} \alpha_{11} & \alpha_{12} & \alpha_{13} & 1 \\ \alpha_{21} & \alpha_{22} & \alpha_{23} & 1 \\ \alpha_{31} & \alpha_{32} & \alpha_{33} & 1 \\ \alpha_{41} & \alpha_{42} & \alpha_{43} & 1 \end{bmatrix} \begin{bmatrix} \delta x_u \\ \delta y_u \\ \delta z_u \\ \delta b_u \end{bmatrix} \qquad (2.8)$$

$$\alpha_{i1} = \frac{x_i - x_u}{\rho_i - b_u} \qquad \alpha_{i2} = \frac{y_i - y_u}{\rho_i - b_u} \qquad \alpha_{i3} = \frac{z_i - z_u}{\rho_i - b_u} \qquad (2.9)$$

From the matrix listed above, the solution can be expressed as:

$$\begin{bmatrix} \delta x_u \\ \delta y_u \\ \delta z_u \\ \delta b_u \end{bmatrix} = \begin{bmatrix} \alpha_{11} & \alpha_{12} & \alpha_{13} & 1 \\ \alpha_{21} & \alpha_{22} & \alpha_{23} & 1 \\ \alpha_{31} & \alpha_{32} & \alpha_{33} & 1 \\ \alpha_{41} & \alpha_{42} & \alpha_{43} & 1 \end{bmatrix}^{-1} \begin{bmatrix} \delta \rho_1 \\ \delta \rho_2 \\ \delta \rho_3 \\ \delta \rho_4 \end{bmatrix} \qquad (2.10)\ [9]$$

As discussed above, the solution obtained for the unknowns still needs the iterative method to find out the final acceptable solution for the location and the value which can terminate the iterative procedure is as the following:

$$\delta x_u = \sqrt{\delta {x_u}^2 + \delta {y_u}^2 + \delta {z_u}^2 + \delta {b_u}^2} \qquad (2.11)$$

In general, the location of the user can be obtained use the pseudorange from 4 satellites or more.

When the receiver can obtain the pseudorange from more than 4 satellites, all of the information will be utilized to find out the location similar to 4 satellites scenario. If we have more than 4 satellites, the equation (2.6) is the same as before:

$$\rho_i = \sqrt{(x_i - x_u)^2 + (y_i - y_u)^2 + (z_i - z_u)^2} + b_u \qquad (2.12)\ [9]$$

The only difference is the matrix of the 4 satellites (2.8) can be expanded as the following:

$$\begin{bmatrix} \delta \rho_1 \\ \delta \rho_2 \\ \delta \rho_3 \\ \delta \rho_4 \\ \vdots \\ \delta \rho_n \end{bmatrix} = \begin{bmatrix} \alpha_{11} & \alpha_{12} & \alpha_{13} & 1 \\ \alpha_{21} & \alpha_{22} & \alpha_{23} & 1 \\ \alpha_{31} & \alpha_{32} & \alpha_{33} & 1 \\ \alpha_{41} & \alpha_{42} & \alpha_{43} & 1 \\ \vdots & \vdots & \vdots & \vdots \\ \alpha_{n1} & \alpha_{n2} & \alpha_{n3} & \alpha_{n4} \end{bmatrix} \begin{bmatrix} \delta x_u \\ \delta y_u \\ \delta z_u \\ \delta b_u \end{bmatrix} \qquad (2.13)\ [9]$$

$$\alpha_{i1} = \frac{x_i - x_u}{\rho_i - b_u} \qquad \alpha_{i2} = \frac{y_i - y_u}{\rho_i - b_u} \qquad \alpha_{i3} = \frac{z_i - z_u}{\rho_i - b_u} \quad (2.14)$$

And (2.13) can be expressed as:

$$\delta\rho = \alpha\delta x \quad (2.15)\ [9]$$

$$\delta\rho = \begin{bmatrix} \delta\rho_1 \\ \delta\rho_2 \\ \delta\rho_3 \\ \delta\rho_4 \\ \vdots \\ \delta\rho_n \end{bmatrix}, \delta x = \begin{bmatrix} \delta x_u \\ \delta y_u \\ \delta z_u \\ \delta b_u \end{bmatrix}, \alpha = \begin{bmatrix} \alpha_{11} & \alpha_{12} & \alpha_{13} & 1 \\ \alpha_{21} & \alpha_{22} & \alpha_{23} & 1 \\ \alpha_{31} & \alpha_{32} & \alpha_{33} & 1 \\ \alpha_{41} & \alpha_{42} & \alpha_{43} & 1 \\ \vdots & \vdots & \vdots & \vdots \\ \alpha_{n1} & \alpha_{n2} & \alpha_{n3} & \alpha_{n4} \end{bmatrix}$$

δρ, δx are both vectors and α is the matrix:

$$\delta\rho = [\delta\rho_1 \quad \delta\rho_2 \quad \dots \quad \delta\rho_n]^T$$

$$\delta x = [\delta x_u \quad \delta y_u \quad \delta z_u \quad \delta b_n]^T$$

$$\alpha = \begin{bmatrix} \alpha_{11} & \alpha_{12} & \alpha_{13} & 1 \\ \alpha_{21} & \alpha_{22} & \alpha_{23} & 1 \\ \alpha_{31} & \alpha_{32} & \alpha_{33} & 1 \\ \alpha_{41} & \alpha_{42} & \alpha_{43} & 1 \\ \vdots & \vdots & \vdots & \vdots \\ \alpha_{n1} & \alpha_{n2} & \alpha_{n3} & \alpha_{n4} \end{bmatrix} \quad (2.16)\ [9]$$

The solution of the equation above can be expressed as:

$$\delta x = [\alpha^T \alpha]^{-1} \alpha^T \delta\rho \quad (2.17)\ [9]$$

δx can be solved using least square estimation. It has the better solution as we have more known values than just using 4 satellites [9].

As we have more known values than before, the iterative method used for equation 2.10 will be also applied to 2.17, the difference is the repeating times of the iterative methods

can be vastly reduced as 2.17 uses least square estimation which converge the final solution much faster, less than 10 iterations [9].

II.5 User location in spherical coordinate system and DOP

The previous part of calculating the user position is based on cartesian coordinates. Actaully the earth itself is not an ideal sphere.

The user location is expressed in longitude, latitude and height. Longitude is centered at the equator from -90 degree to 90 degree and latitude is centered at prime meridian in Greenwich Observatory, ranging from -180 degrees to 180 degrees. The height is just the latitude from the surface of the earth [9].

User p is located at (x_u, y_u, z_u). The distance d from the center of the sphere to the user p is just [9]:

$$d = \sqrt{{x_u}^2 + {y_u}^2 + {z_u}^2} \quad (2.18)$$

The altitude L is:

$$L = \tan^{-1}\left(\frac{z_u}{\sqrt{x_u^2+y_u^2}}\right) \quad (2.19)\ [9]$$

The longitude l is:

$$l = \tan^{-1}(\frac{y_u}{x_u}) \qquad (2.20)\ [9]$$

The height h is, where r_e is the radius of the earth.

$$h = r - r_e \qquad (2.21)\ [9]$$

Obviously when calculating the user position, some conversions are needed to transform from the Cartesian coordinates to spherical coordinates. There are lots of further discussion about how to determine the location as the earth is not an ideal sphere, in this thesis, we are not focusing on the coordinate system conversion. If interested, several good references are given [10].

The term dilution of precision (DOP) is used to describe the precision of measuring the user location [10]. The DOP depends on the geometry of the distribution of the satellites in the sky, in reference [10], it has the detailed discussion of how to calculate the DOP. In this thesis, only the definition will be given as:

$$\text{GDOP} = \frac{1}{\sigma}\sqrt{\sigma_x^2 + \sigma_y^2 + \sigma_z^2 + \sigma_b^2} \quad (2.22)\ [9]$$

σ is the root mean square errors of the pseudorange.

$\sigma_x, \sigma_y, \sigma_z$ are the root mean square errors on the xyz directions.

σ_b is just the root mean square error of the user clock [9].

The 3D dilution of precision PDOP is defined as:

$$\text{PDOP} = \frac{1}{\sigma}\sqrt{\sigma_x^2 + \sigma_y^2 + \sigma_z^2} \qquad (2.23)\ [9]$$

The 2D dilution of precision HDOP is [9]:

$$\text{HDOP} = \frac{1}{\sigma}\sqrt{\sigma_x^2 + \sigma_y^2} \qquad (2.24)\ [9]$$

And the vertical dilution of precision VDOP is [9]:

$$\text{VDOP} = \frac{\sigma_z}{\sigma} \qquad (2.25)\ [9]$$

And the time dilution of precision TDOP is [9]:

$$\text{TDOP} = \frac{\sigma_b}{\sigma} \qquad (2.26)\ [9]$$

The smaller the DOP is, the better geometry the user select the satellites as demonstrated as in Figure 2-4 and 2-5:

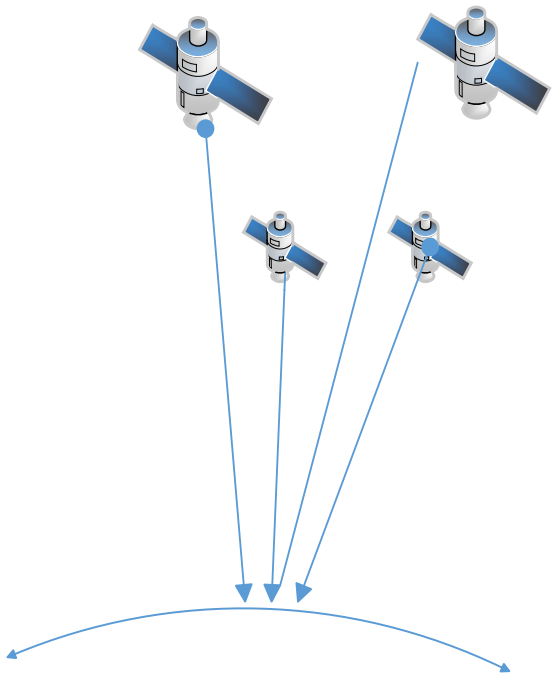

Figure 2-4 Poor DOP [11]

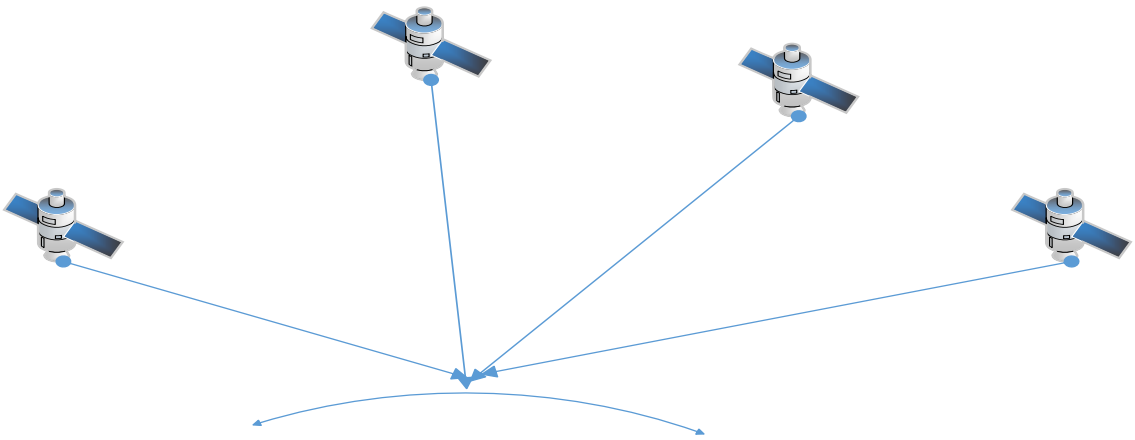

Figure 2-5 Good DOP [11]

The good DOP proves that the coverage volume of the space is the maximized [11]

CHAPTER III

EXPERIMENT SETUP

III.1 Introduction

In this chapter, the details of setting up the experimental platform and designing various experiments to test the performance of the SDR will be demonstrated.

This chapter includes more descriptions of the software and hardware architecture and how this architecture can affect the measurement of the GNSS real time signals. The purpose of each experiment will also be discussed to ensure the data collected were valid and ready to analyze. Also, every part of the experiment platform will be displayed and explained.

III.2 Setup the hardware experimental platform

The overall system setup is shown as Figure 3-1:

Here is the list of the parts on the platform:

A. Power supply or battery pack
B. Ethernet connection with host computer
C. Bias tee with a constant voltage supply
D. USRP with daughterboard and GPS clock kit
E. Active antenna

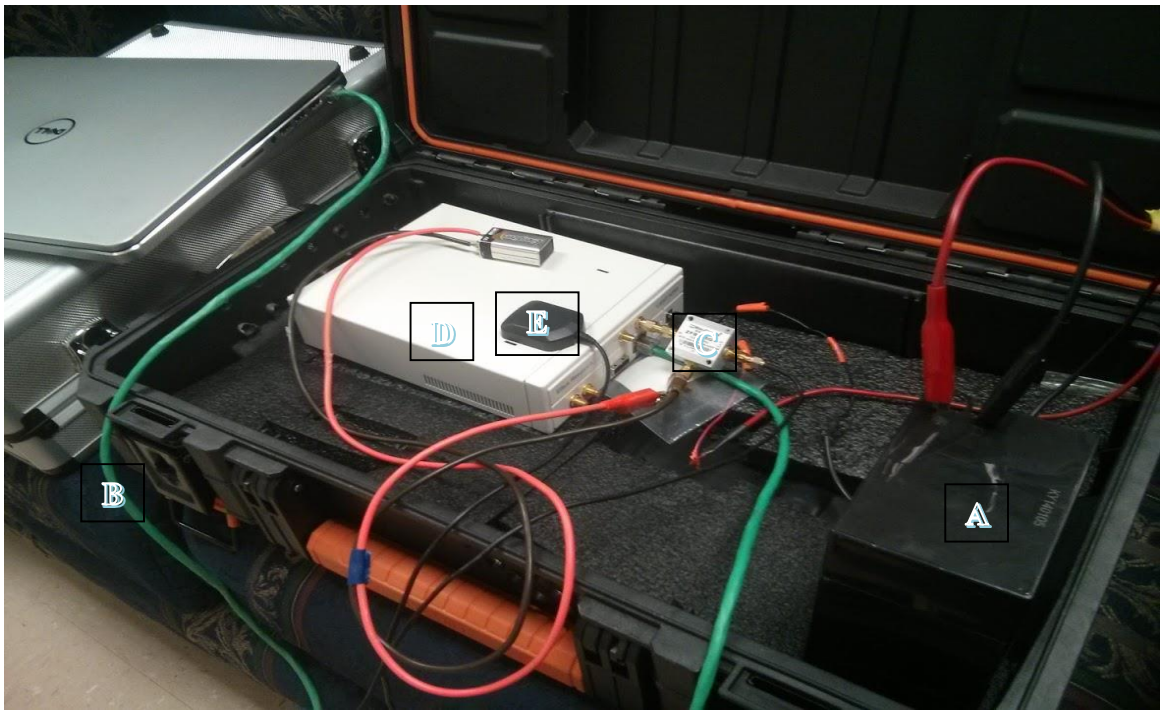

Figure 3-1 Hardware setup for the experiment platform

Part A: Power supply or battery pack

We use a 9V battery to connect the bias-tee which connects to the RF2 port of USRP. The power supply can be either from a plug which can provide normally 6V 3A to the USRP or we can use an external battery pack, which can last from 2 hours to 4 hours based on its capacity. On the experimental platform, battery WKA6-14A and WKA6-12F were used.

For WKA6-12f, under 6V and discharging rate at 3A, the total time of discharging is approximately 2 hours, while for WKA6-14a, the discharging time is more than 3 hours.

But 2 – 3 hours is not sufficient for the whole day test, so some experiments which can observe the periodicity of the satellites can be modified to a certain time frame of the day to detect the same sets of satellites.

For some field experiments, while there is no power plug available, the battery is the only power source for the experiment. Some interesting effects were noted during the experiment using the external battery pack. The pseudorange which was obtained from the experiment sometimes has the abrupt drift from the graph and bounce back after some time, the assumption made here is the battery pack sometimes fails to deliver enough current to the SDR, when the clock of SDR wasn't stabilized, it would lead to transient errors. That being said, the majority of the psudeorange measurement are not affected.

Part B: Ethernet connection with host computer

The Ethernet cable is just the connection between the computer and USRP N200.

Part C: Bias tee with constant voltage supply

Here is another picture of the bias-tee with the battery in Figure 3-2：

Figure 3-2 Bias-tee with battery

Our experiment requires the receiver to keep a low noise figure. The GNSS antenna itself has integrated a low noise amplifier (LNA) which can provide a GNSS signal gain for the daughterboard [22]. The bias-tee can achieve the goal that the desired signal can be amplified before attenuated by other components. In this experiment, ZFBT-6G+ is utilized.

There are two general approaches to provide DC power to the LNA integrated in the antenna. One is the daughterboard can internally provide the power. The other is to connect bias-tee with the independent power supply. In our field test, the battery is

utilized. The bias-tee itself acts as the RF signal path which also isolates the input DC component, which always requires a capacitor to AC couple the signal as the following model:

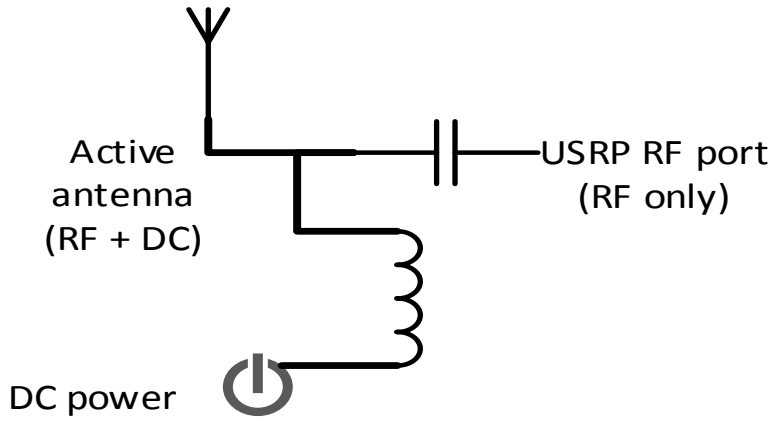

Figure 3-3 Schematic of a bias-tee [12]

Part D: USRP with daughterboard and GPS clock kit

The following Figure 3-4 and Table 3-1 displays the GPSDO kits used to stabilize the clock in the experiment and its specifications:

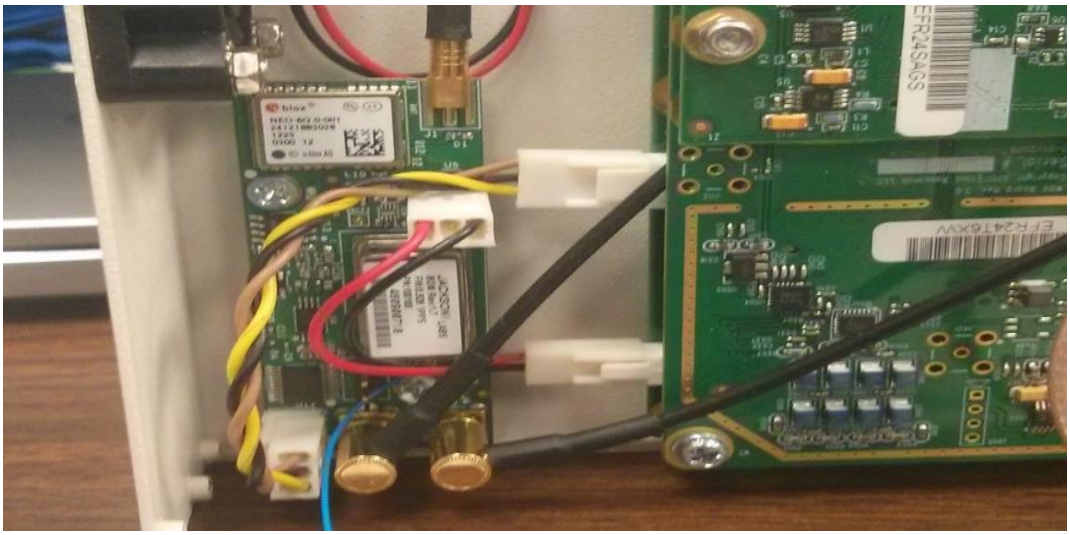

Figure 3-4 GPSDO kits

GPSDO Module Specifications	
1 PPS accuracy	50ns to UTC RMS (1-sigma) GPS locked
GPS Frequency	L1,C/A 1574MHz
GPS Antenna	Active (5V compatible) or passive
Sensitivity	Acquisition -142 dBm, Tracking -168 dBm
TTFF	Cold Start: < 45 sec, Warm Start: 1 sec, Hot Start: 1 sec
Warm Up Time / Stabilization Time	<5 min at 25C to 1E-08 Accuracy
GPS Receiver	50 channels, Mobile, WAAS, EGNOS, MSAS capable

Table 3-1 Module Specification of GPSDO [13]

The RF daughterboard used in the experiment is WBX, which is a wide bandwidth

transceiver providing up to 100mW of power and its noise figure is 5dB. WBX can provide 40MHz of bandwidth capacity and ranges from 50MHz to 2.2GHz, which means that the 1.575GHz GPS signals can be successfully sampled using WBX. WBX daughterboard also features 2 quadrature front ends, one for transmitting signal, one for receiving the signal. The transmit antenna can be TX/RX port, while the receive antenna can be appended to TX/RX or RX2 port.

The following Figure 3-5 shows the WBX daughterboard used in the experiments:

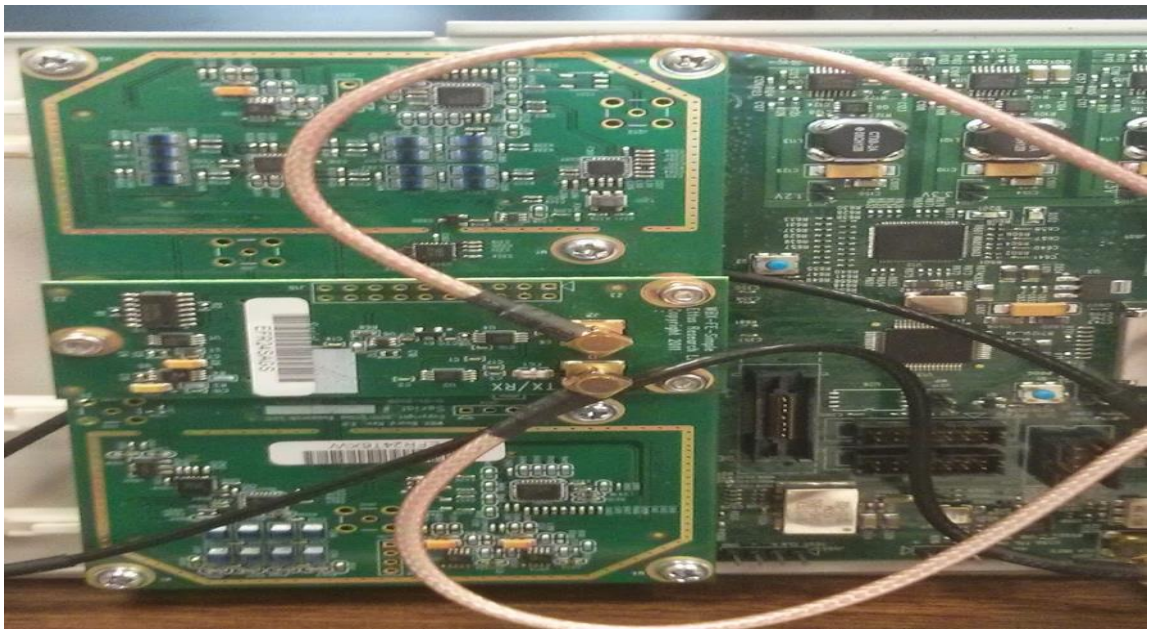

Figure 3-5 WBX daughterboard

III.3 Setup the software experimental platform

To connect to the host computer, the Ethernet cable needs to be plugged in and open the Ubuntu terminal to input the command to set the USRP to Ethernet IP address:
sudo ifconfig eth0 192.168.10.1
The detailed set of commands can be found at
http://files.ettus.com/manual/page_usrp2.html [23].

One important thing about the Ubuntu Ethernet connection is that, the network manager can manage the Ethernet port as the DHCP port which resets the connection with the USRP N200. If the connection is constantly lost, we either can use the Linux command to give the Ethernet port with the constant IP address or directly disable the network manager of controlling the Ethernet connection to let the network manager ignore the connection with USRP.

If we wish to check if there are any GNSS signals available for the antenna, we can open GRC which is the graphical user interface for GNU radio and open the file in
/gnuradio/gnuradio/gr-uhd/examples/grc/uhd_fft.grc
After we set the center frequency to 1.575E09 Hz, if there are any GPS signals available, with the bias tee attached. The waterfall diagram obtained from GNU Radio may have several brighter colored yellow lines around the center frequency as in Figure 3-6:

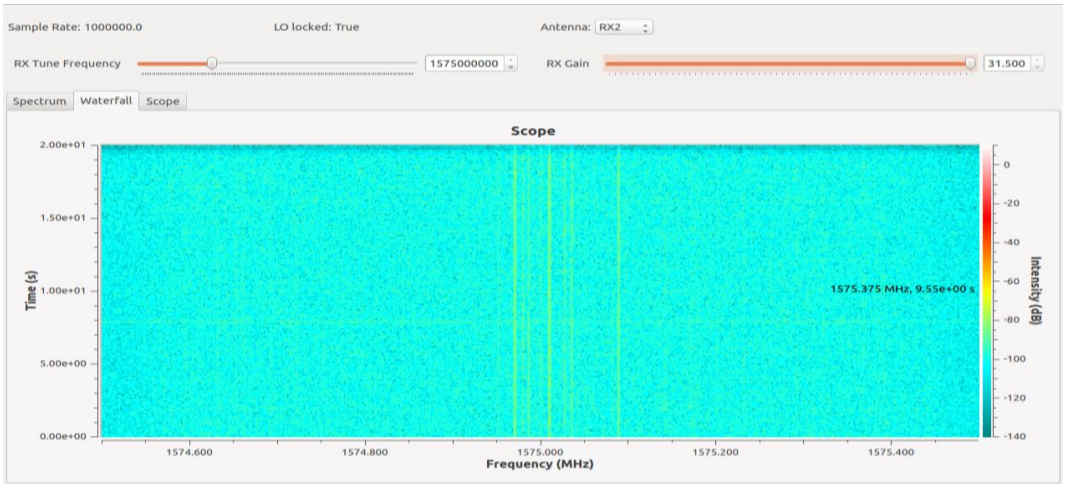

Figure 3-6 Waterfall

In Figure 3-7 are the diagrams for the spectrum and scope of the GNSS signals：

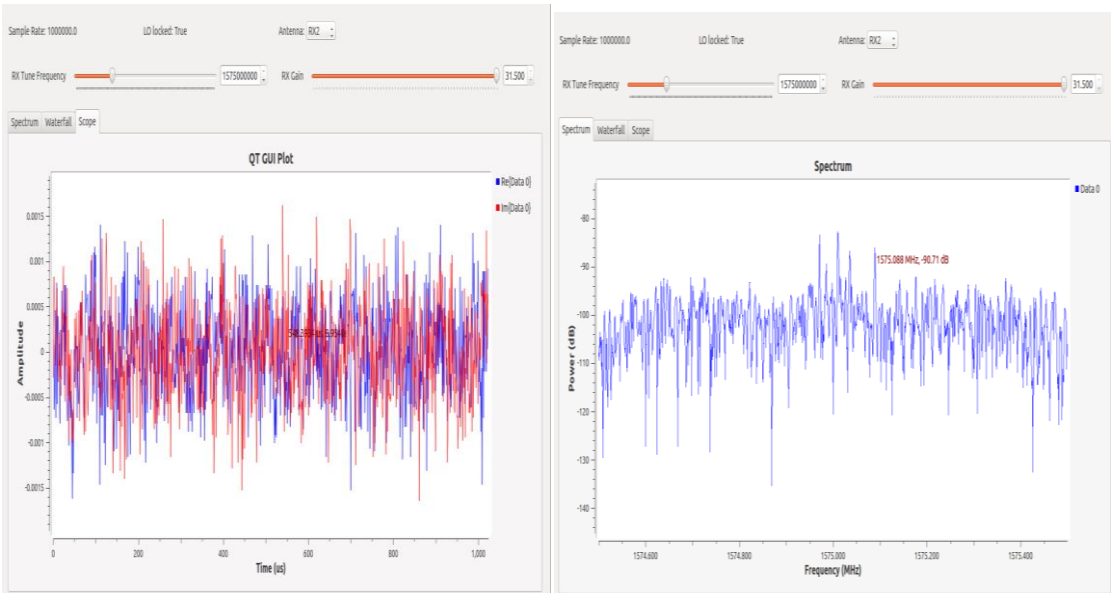

Figure 3-7 Spectrum and scope of the signal

To designate the USRP as a GNSS receiver, the software package has to be installed and for this particular application, we use GNSS-SDR. The official website is: www.gnss-sdr.org and the setup procedure can be referred to the documentation on the website.

One thing need to mention here is that there are two ways to install GNU Radio or UHD driver. One is to use the Python Build Overlay Managed Bundle System (PyBOMBS), it automatically installs the software needed for GNSS-SDR such as GNU Radio, UHD, rtl-sdr etc. The other way is to manually install each software according to their manuals, this process is tedious but can ensure that each software can be installed correctly as each bundle of software can have several versions, manually installing the software can make sure the version is concurrent with other software bundles.

If the software is set up correctly, we can open the Ubuntu terminal again and change to the /home/rtds/gnuradio/gnss-sdr/install.

To use the GNSS-SDR software, we can choose a configuration file inside folder /home/rtds/gnuradio/gnss-sdr/conf

And input the command: gnss-sdr –config_file=gnss-sdr_GPS_L1_USRP_realtime.conf, here we use a configuration file designated for GPS L1 signals. We can also use the hybrid mode configuration file which is gnss-sdr_hybrid which can acquire both the Galileo and GPS signals and utilize the information acquired from both GNSS system and combine them to generate the RINEX file to help locating the position, one of the

experiment is designated to conduct this hybrid system experiment in Chapter IV.

If the configuration file needs the assisted GPS (A-GPS), this line of script can be set to be true to read the XML assisted GPS file to the C++ modules like below:

GNSS-SDR.SUPL_gps_enabled=true

For USRP N200, the device target should be set to A:0:

;#subdevice: UHD subdevice specification (for USRP1 use A:0 or B:0)

SignalSource.subdevice= A:0

If the GPS channels needs to be set to track the particular satellites, we can use the following example to write:

;######### SPECIFIC CHANNELS CONFIG ######

;#The following options are specific to each channel and overwrite the generic options

;######### CHANNEL 0 CONFIG ############

;Channel0.system=GPS

;Channel0.signal=1C

;#satellite: Satellite PRN ID for this channel. Disable this option to random search

;Channel0.satellite=11

;######### CHANNEL 1 CONFIG ############

;Channel1.system=GPS

;Channel1.signal=1C

;Channel1.satellite=18

The channels can be configured to lock to a particular satellite.

When the software starts working, the console from the Ubuntu will output which satellites' navigation information is ready and the longitude and latitude of the position

Figure 3-8 is the general diagram of the software. The software itself has two very important planes. One of them is control plane illustrated in Figure 3-8 as GNSSFlowgraph block. It is in charge of creating a flow graph. User can define customer receiver by changing the functions of the control plane. Another plane is signal processing plane which can implement signal processing functions and define implementations according to configuration file which can integrate into GNSSBlockInterface in Figure 3-8.

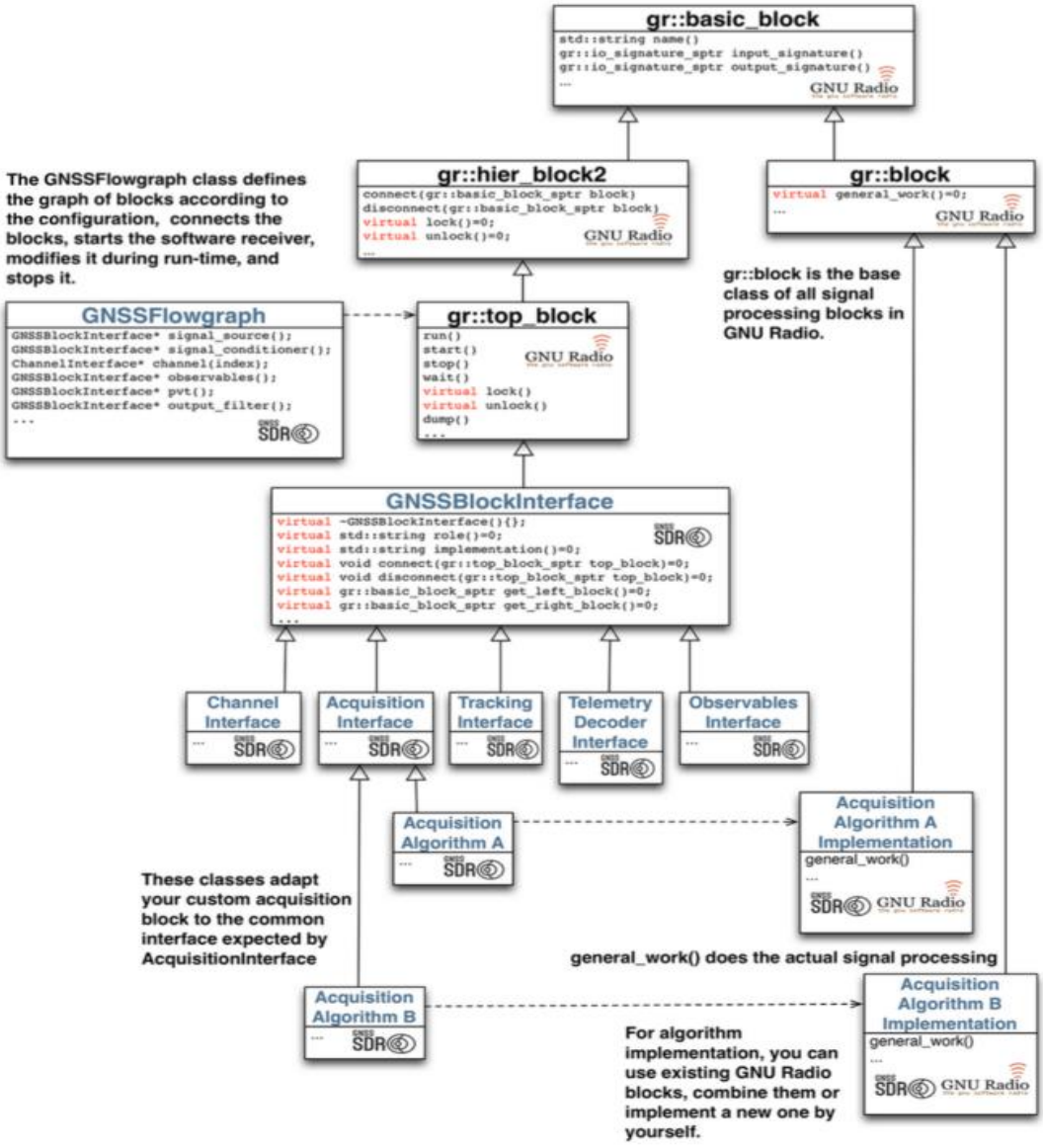

Figure 3-8 General UML diagram [2]

CHAPTER IV

EXPERIMENT DESIGN AND ANALYSIS

IV.1 Introduction

This chapter contains all the verification of the assumptions proposed before. The data collection part was carried out on several locations both on campus of Texas A&M or off campus, so that the results can be more robust. The experiment proposed and designed can help illustrate how well the signal reception is for our research platform which takes into account of various factors such as weather, algorithms of calculating PVT, pseudorange quality and multipath in urban canyons. By conducting these experiments, the quality of the signal reception of this research platform was fully investigated so that in the future the researchers can have a better sense of how well this platform can contribute to the GNSS research and why using this platform can save time and increase the efficiency of validating assumptions and ideas.

IV.2 Experiment motivations

The experiment listed in this chapter mainly focuses on those factors which can contribute to the GNSS location precision and error. The results obtained from the experiments can help us better understand the performance and limitations of this research platform. Here is the list of the possible error factors and possible comparison experiments can be conducted in Table 4-1.

Source	Error Distribution [m]	Difference with
Ionosphere delays	10	CORS
Troposphere delays	1	weather
PRN Code Noise	1	N/A
SV Clock	1	model correction/post-processing
SV Ephemeris Data	1	model correction/post-processing
Psuedo-Ranqe Noise	1	N/A
Receiver Noise	1	signal
Multipath Error	0.5	no blocking condition
Numerical behavior	5	Intermediate Results
Typical Error with Basic GPS	15	Actual Location

Table 4-1 GNSS error source [24]

IV.3 Experiment design and statistics

The basic procedures of conducting an experiment is listed below in Figure 4-1:

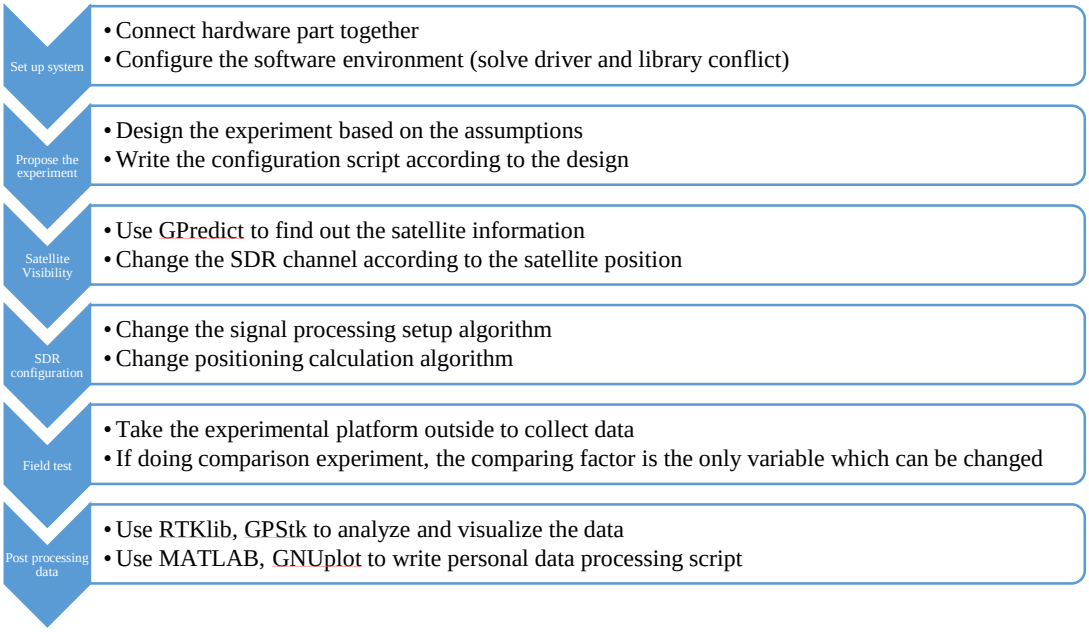

Figure 4- 1 Experimental procedure

The major performance criteria consist of two parts, Figure 4-2 can demonstrate the relationship between them.

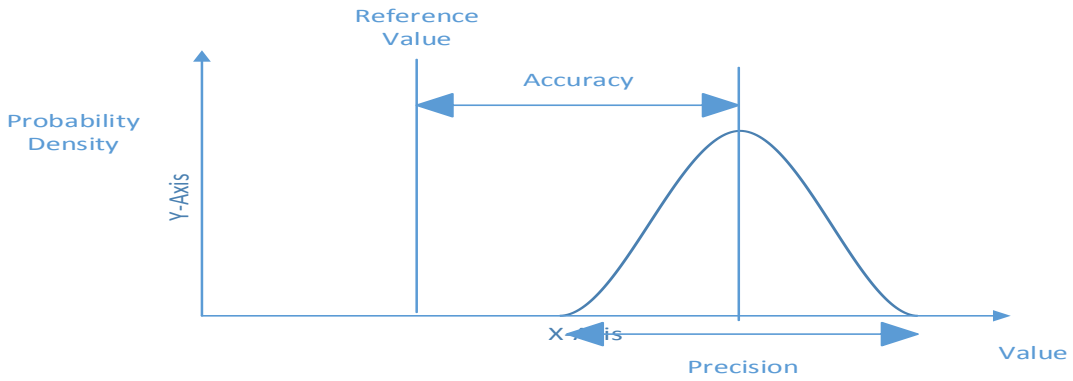

Figure 4-2 Accuracy VS Precision [21]

The precision has the mean value which is not the reference value. The difference between them is the accuracy.

To describe the precision of the value measured, several statistical terms will be used as below:

DRMS: It is the root mean square of the squared x, y direction (longitude, latitude) errors, which is $\sqrt{\sigma_x^2+\sigma_y^2}$ meaning 65% of the points are in DRMS circle.

2DRMS: It is twice the DRMS of the x, y direction (longitude, latitude) errors which is $2\sqrt{\sigma_x^2+\sigma_y^2}$ meaning 95% of the points are in 2DRMS circle.

CEP: It is the radius of a circle centered at the average of the points containing 50% of the measured position points which are equal to $0.56\sigma_x + 0.62\sigma_y$.

Delta (latitude, longitude): The difference of the measured average longitude and latitude to the actual SDR's latitude and longitude in meters. In the following experiment, latitude and longitude also represent north and east measurement.

IV.4 Compare software defined radio with Continuously Operating Reference Station (CORS)

Aim: This experiment aims to find out the performance of software defined radio in a field test with CORS as well as the ionosphere effect on positioning. CORS information is downloadable online including its RINEX files, coordinates, log files and IGS ephemeris.

Method: The SDR was placed around 50 meters from the CORS satellite and its RINEX file was also saved. Both CORS and SDR has no blocking from buildings or trees so that this experiment is free from multipath transmission.

Results and analysis: In Figure 4-3 shows the comparison of the pseudorange for SDR on the left and CORS on the right, the pseudorange plot below was obtained from the SDR and CORS RINEX file, x-axis is the point number, y axis is the pseudorange in 10^7 meters.

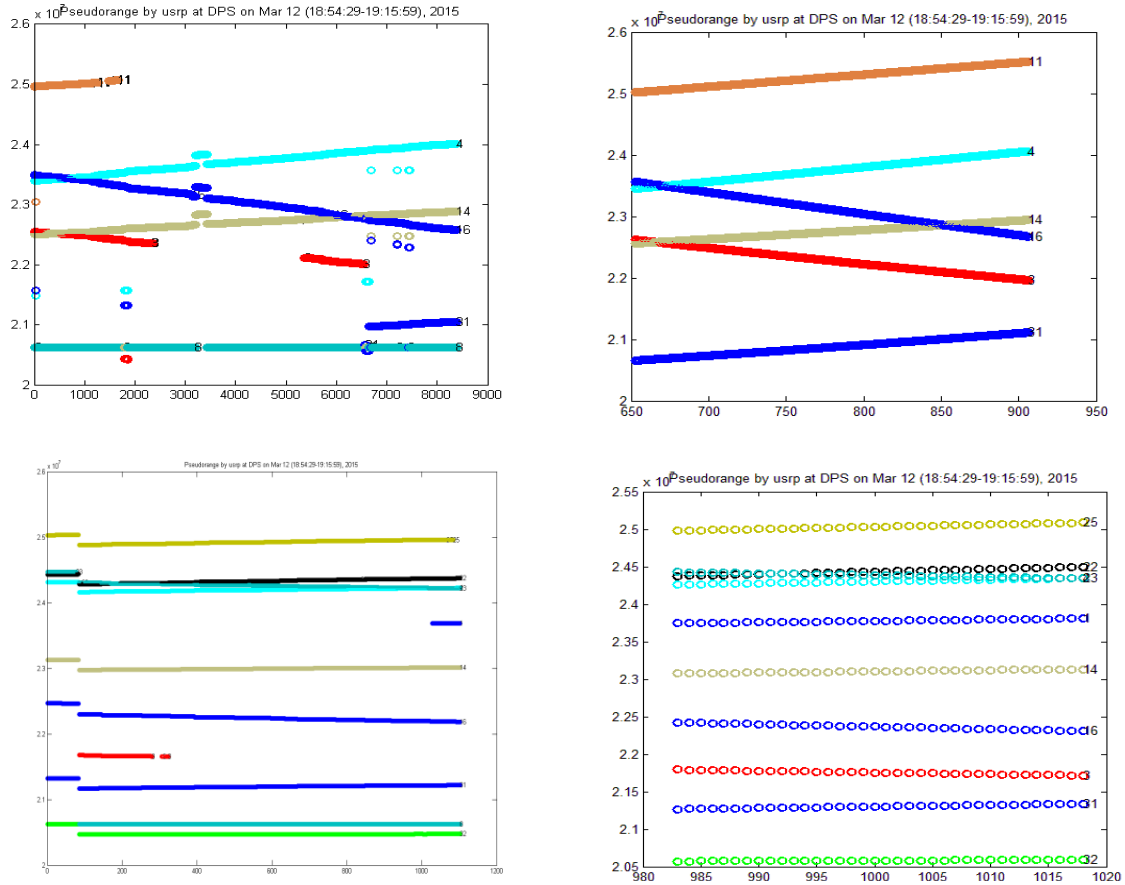

Figure 4-3 Pseudorange comparison USRP and CORS

From the first comparison in Figure 4-3, it is possible that the USRP still has some clock drifting issues which create some gaps in the pseudorange as all the pseudorange drifts at the same time. These clock drifts may impact the final position calculated using the algorithm in GNSS-SDR, but it can also be modified and adjusted using some open source software to move the points which are ambiguous. In the second comparison in Figure 4-3, the SDR has some gap in the pseudorange at initialization, which possibly means the acquisition algorithm need to initialize the data collected first. Also data collected from SDR is denser then CORS data on the diagram. The increment for SDR are 0.1 second while CORS is 1 second. From the Google Earth plot, it is clear that due to some pseudorange drift shown in Figure 4-3, the positioning of the SDR also sometimes drifts away from the actual location. But most of the time, the positioning of the SDR is within 10 meters from the actual location displayed as yellow arrow in Figure 4-4.

Figure 4-4 Google Earth location plot near DOT

IV.5 Effect of weather

Aim: This experiment is designed to find out if the weather can contribute to the accuracy and precision of the GNSS SDR, when the weather is cloudy, the troposphere can add the signal path length to the receiver, without the corrections on this factor, the experimental results can be quite different when the weather is sunny (low troposphere effect) or when the weather is cloudy (high troposphere effect) [14].

Figure 4-5 Weather sunny (left) cloudy (right)

Method: Place the SDR on the rooftop of HRBB (computer science and engineering) and record the GNSS data for 5 minutes. The rooftop has no blocking of viewing the satellites in the sky and the weather. Record GNSS data in different weather condition, sunny or cloudy as Figure 4-5 shows.

Results and analysis: The overall scatter points on Google Earth for both sunny and cloudy weather is in Figure 4-6 and the red line is the cloudy weather, green line is the sunny weather:

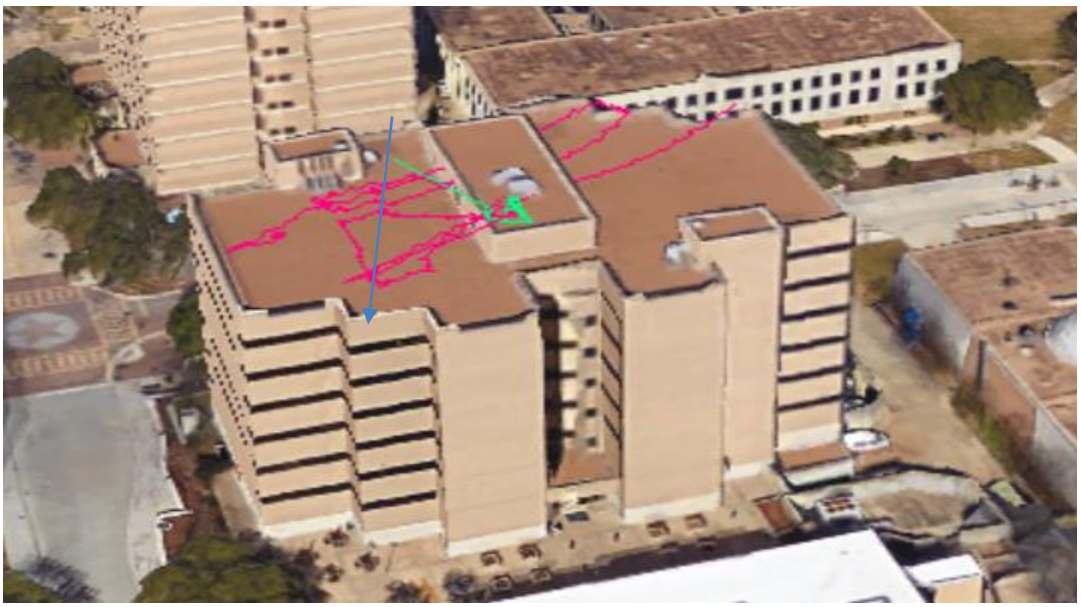

Figure 4-6 Google Earth plot weather effect

From Figure 4-6, it is clear that in cloudy weather the calculated location is varying more than in good weather. In Figure 4-7, the longitude and latitude data are converted to east and north position in meters and plotted to demonstrate the how big the varying is on both longitude and latitude. The high troposphere graph is the cloud weather and the low troposphere graph is the sunny weather. From Figure 4-7, the cloudy weather's location data is varying much bigger than the sunny weather's location data.

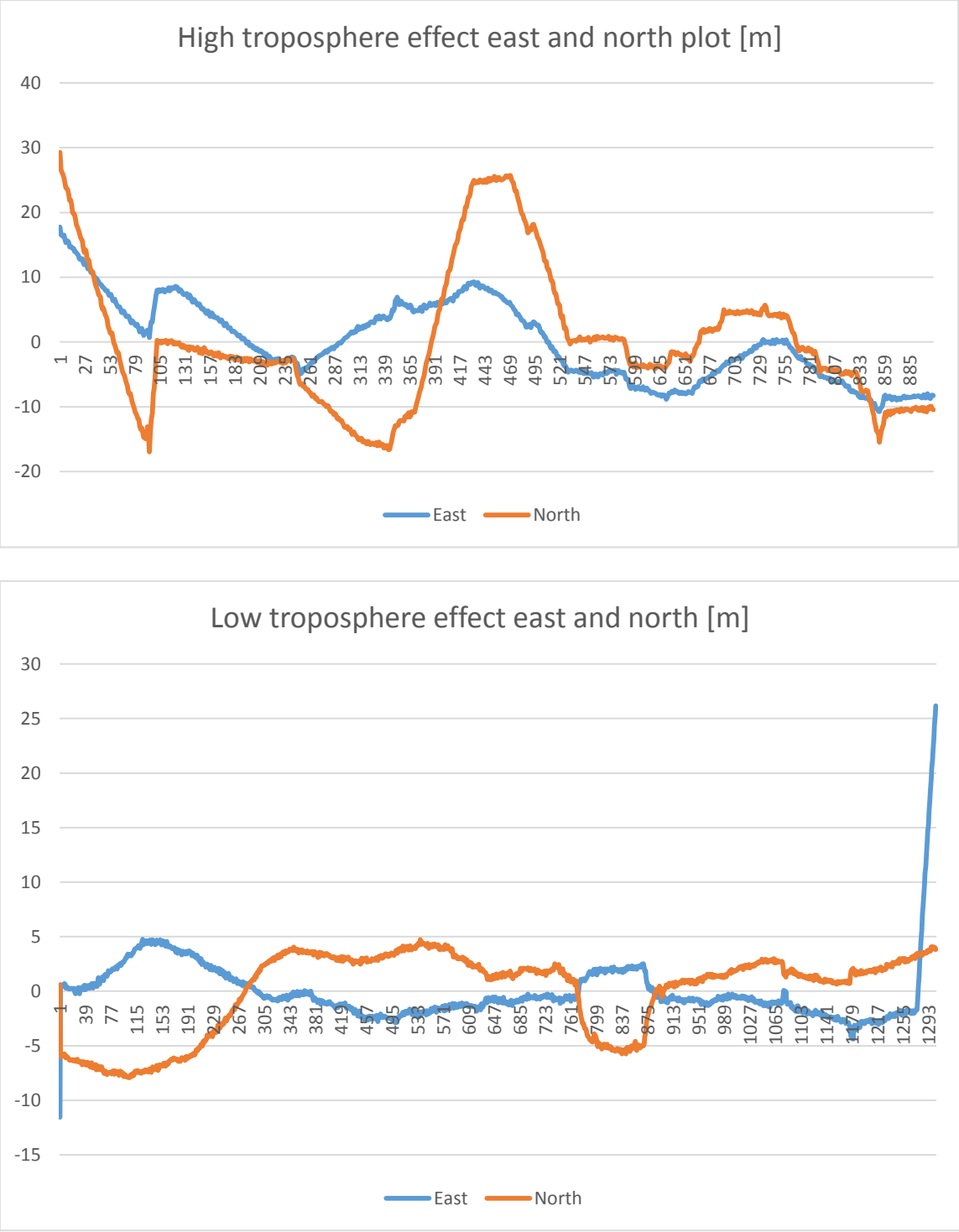

Figure 4-7 East and north plot of weather (0 is their own average)

In Table 4-2, error analysis data in meters are listed:

	Low troposphere effect	High troposphere effect
Standard deviation East	6.12	2.94
Standard deviation North	10.44	3.77
CEP	9.77	3.96
2drms	24.2	9.57
Delta East (to actual)	2.86	8.42
Delta North (to actual)	1.73	7.78

Table 4-2 Statistics analysis effect of weather

From Table 4-2, the standard deviation of longitude and latitude demonstrates that the troposphere can change the precision of the location by around 5 meters in this experiment. In Figure 4-8, the precision scatter plot of the sunny (good weather) and cloudy (bad weather) is shown. From the plot, it is noticed that the troposphere managed to affect the precision of the location in this experiment. It is also observed from Table 4-2 that the delta value of longitude and latitude from the actual location is different. The cloudy weather has a higher accuracy in this experiment. The explanation here is when we located the actual location on Google Map, it wasn't exactly the actually the position of the SDR was placed. This may cause some errors of accuracy.

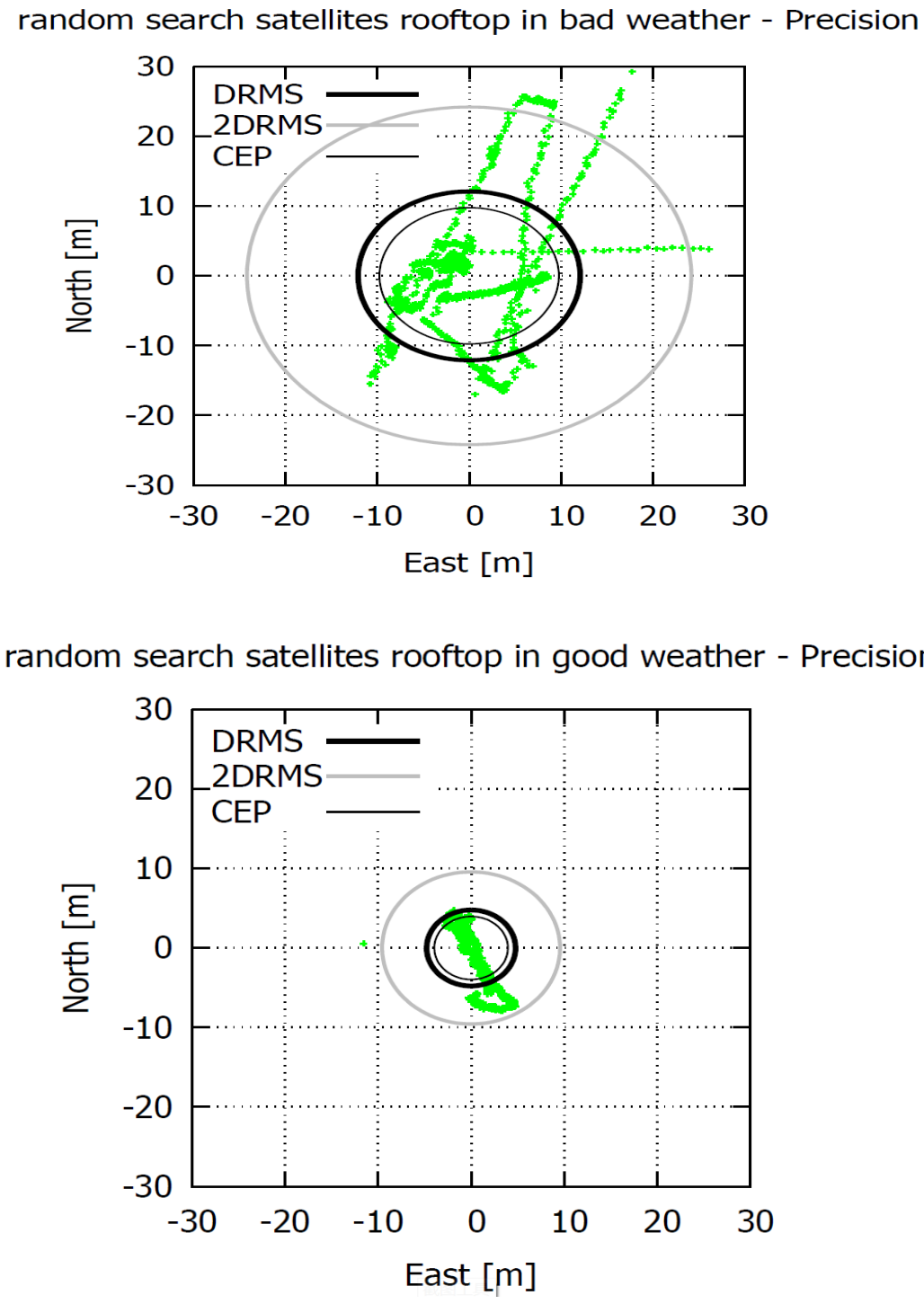

Figure 4-8 Weather precision

IV.6 Effect of Multipath

Introduction: GNSSS data from USRP can be utilized for the improvement of the reception of the signals. For examples, in urban canyons, the GNSS signals can often be blocked by skyscrapers or buildings which leave less available satellites to be detected which cause the multi-path problem [15]. Figure 4-9 depicts such scenario:

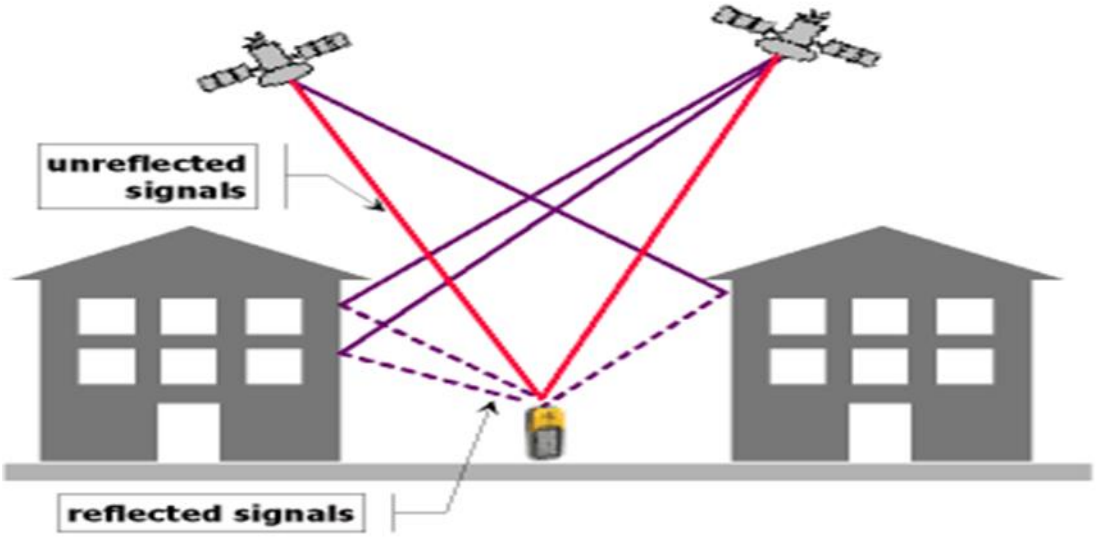

Figure 4-9 Multipath in urban canyon [16]

The direct-path signal from the satellites and the reflected signal from the buildings or rooftops as saw from Figure 4-9 are the two types of signals which the GNSS receiver can acquire.

To solve the multi-path problem, lots of research were conducted on the integrity of signals which compare the multi-path signal and direct-path signal and use the special multipath limiting antennas to reduce the problem [17].

However, in an urban canyon, if the satellite is blocked from the line of sight, no direct-path can be identified, and the only signal acquired from the receiver is just the multipath signal. And the multipath signal couldn't be used as the satellite signal to calculate the position.

Thus, those methods based on the comparison of the direct-path signal couldn't be utilized. Under such circumstances, it is necessary to develop a new methodology to solve the problem of multi-path signal in urban canyons and validate such methodology on software defined radio.

To explain the skyplot, it is an interesting graphic that combines some of the information presented in the other graphics. Basically, the skyplot tracks the movement of satellites in terms of elevation (inclination) and azimuth (North, South, East, West). At various points along each track, one can obtain the hour of the day (in military time) [18]. In Figure 4-10 is the skyplot with the tracks of satellites in an urban canyon.

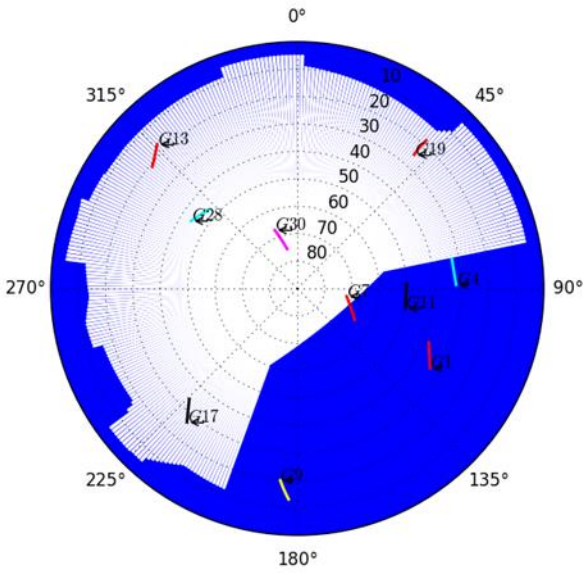

Figure 4-10 Skyplot of satellites

Aim: This experiment is trying to figure out the effect of urban canyon and how the selection of the satellites can reduce this effect. This experiment is quite useful to validate the effectiveness choosing the direct satellite signal.

Method: The input needed for this experiment is the viewshed skyplot as well as the track of each satellites on the skyplot. The viewshed skyplot can be generated using different methods such as fisheye camera to capture the sky in urban canyons [25]. In our case, the viewshed skyplot is obtained using the shape files of the building and the height of each building in the urban canyon.

After obtaining the viewshed skyplot, the experiment can start comparing the accuracy of the receiver by selecting the satellites whose elevation is high enough so that no multipath signal can be generated to reach the receiver or randomly select the satellites which are visible to the receiver. In random selecting case, there is chance that the signal received from the satellite is reflected as the elevation of the satellites is not tall enough to avoid the reflection.

The SDR can be placed inside a small urban canyon on campus and record roughly the same length of data for random selecting satellite case and fixed channel case. The results of the comparison will be displayed on Google Earth, EN graph which can

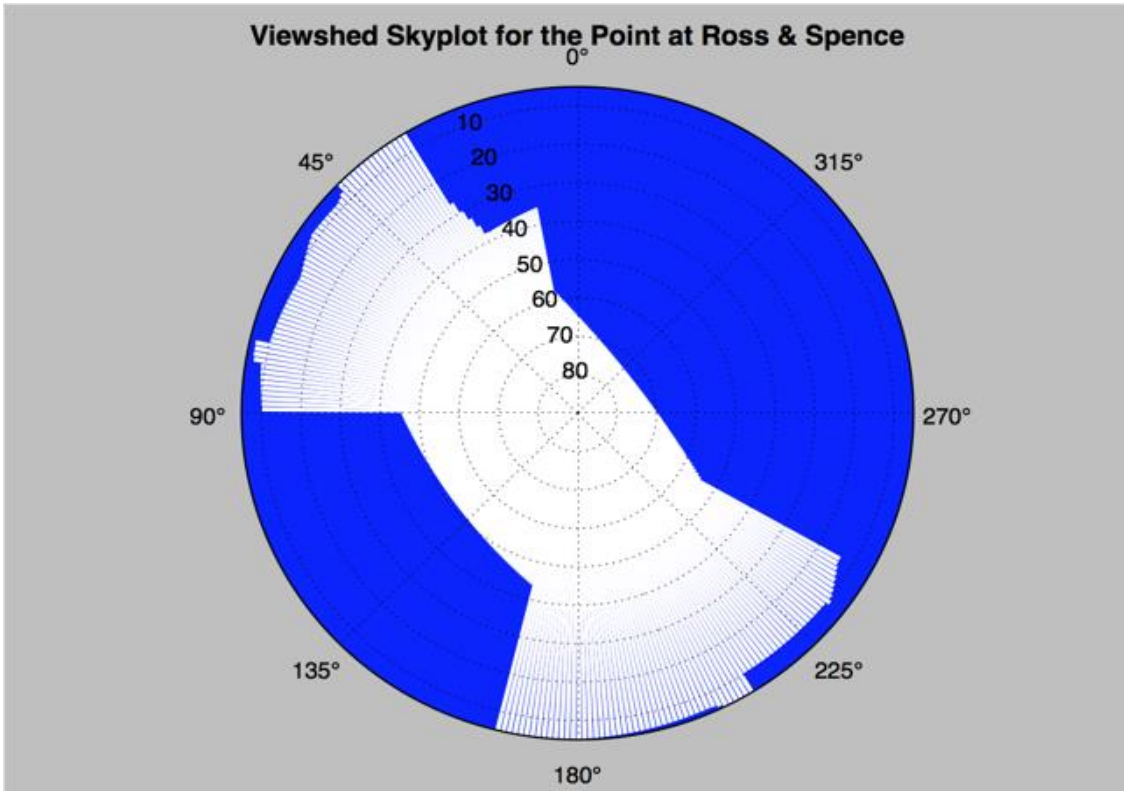

Figure 4-11 Viewshed skyplot near HRBB

demonstrate whether or not selecting the satellites without the concern of multipath would help improve the accuracy and precision of GNSS positioning.

Results: The SDR was placed near the Ross and Spence St. The generated viewshed skyplot from the python code which was implemented is in Figure 4-11. Using random search, the SDR can sometimes capture the signal strength which is above the threshold but below the average of other satellites. This can be an indication of a multipath signal which was reflected and received and this scenario can change the pseudorange measured from the actual satellite thus changes the accuracy and precision of locating the SDR [19].

We did find out some signals may be reflected as they weren't in the viewshed and their signal strength is the lower than the satellites in the viewshed. It is the satellite G4 which is not in the viewshed in Figure 4-12 but still appears in the pseudorange calculations.

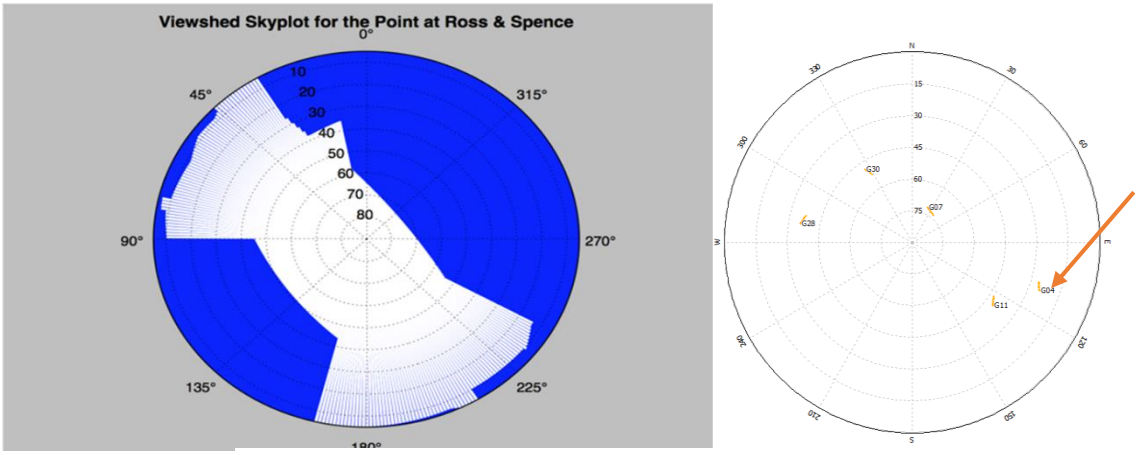

Figure 4-12 Satellite G04 not in viewshed

The arrow points to G4. If we compare the SNR plot generated from RTKlib of G04 left with another satellite G30 right in Figure 4-13.

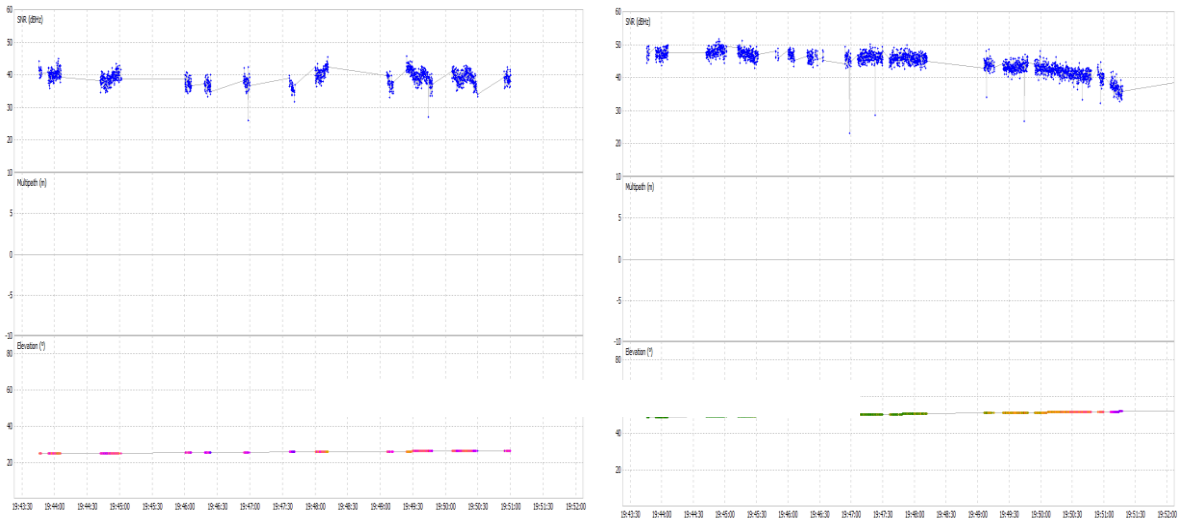

Figure 4-13 SNR comparison

G30 is in the viewshed and its SNR is around 10 dB more than G4 which is not in the viewshed.

Using the random search method, some potential multipath signal can be received and used as the calculation of the position. To fully eliminate such scenario, we can fix the channels of SDR to only receive the signal in the viewshed which means the effect of multipath can be reduced. The detailed setup of random search and fixed channel search can be referred to Chapter 3.

We only selected the satellites which are in the viewshed in Figure 4-14.

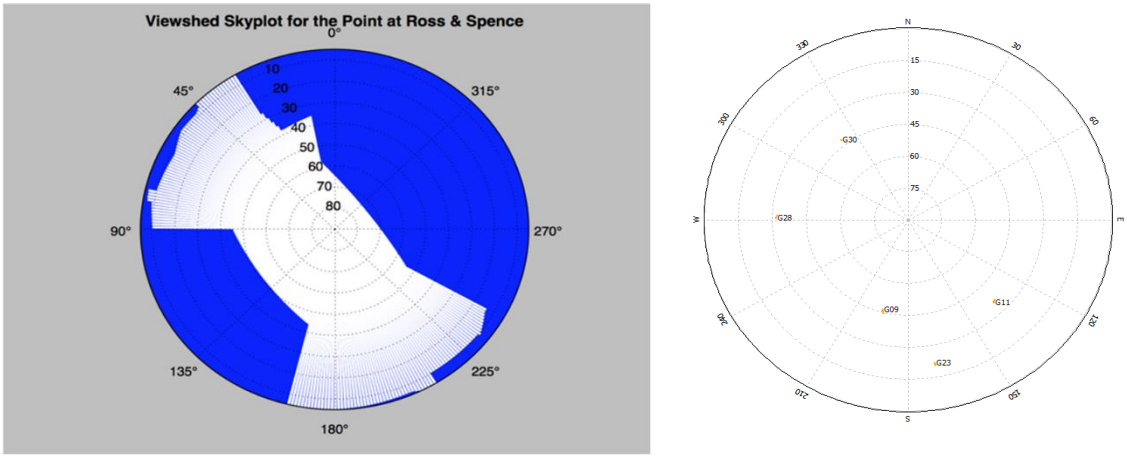

Figure 4-14 Fix channel skyplot

And its SNR plot of a fixed satellite is in Figure 4-15

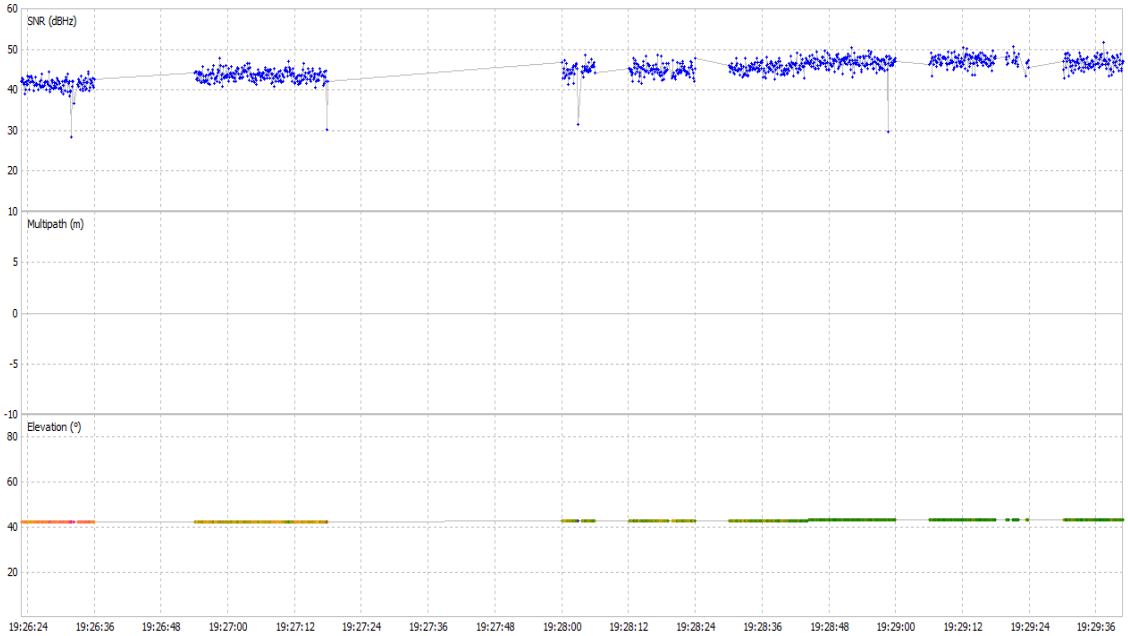

Figure 4-15 SNR fixed channel

The fixed channel method has no suspicious satellite whose signal received can be reflected on the wall or rooftop of buildings and the SNR of the satellites is higher than the SNR of satellites not in the viewshed.

The overall positioning on the Google Earth is as the following, the red line is the result of the random search method which may have multipath effect and the blue line is the fixed channel method solution which has smaller multipath affection, the arrow points to the point where SDR was placed in Figure 4-16.

Figure 4-16 Fixed channel and random search near HRBB

Detailed statistics of the positioning are in Table 4-3.

	Fixed Channel (avoid multipath)	Random Search (possible multipath)
Standard deviation East	2.7	7.8
Standard deviation North	4.5	10.4
CEP	4.3	10.8
2drms	10.5	26.1
Delta East (to actual)	-6.6	-19.7
Delta North (to actual)	-9.58	-55

Table 4-3 Statistics analysis fixed and random search

The East and north position plot is in Figure 4-17:

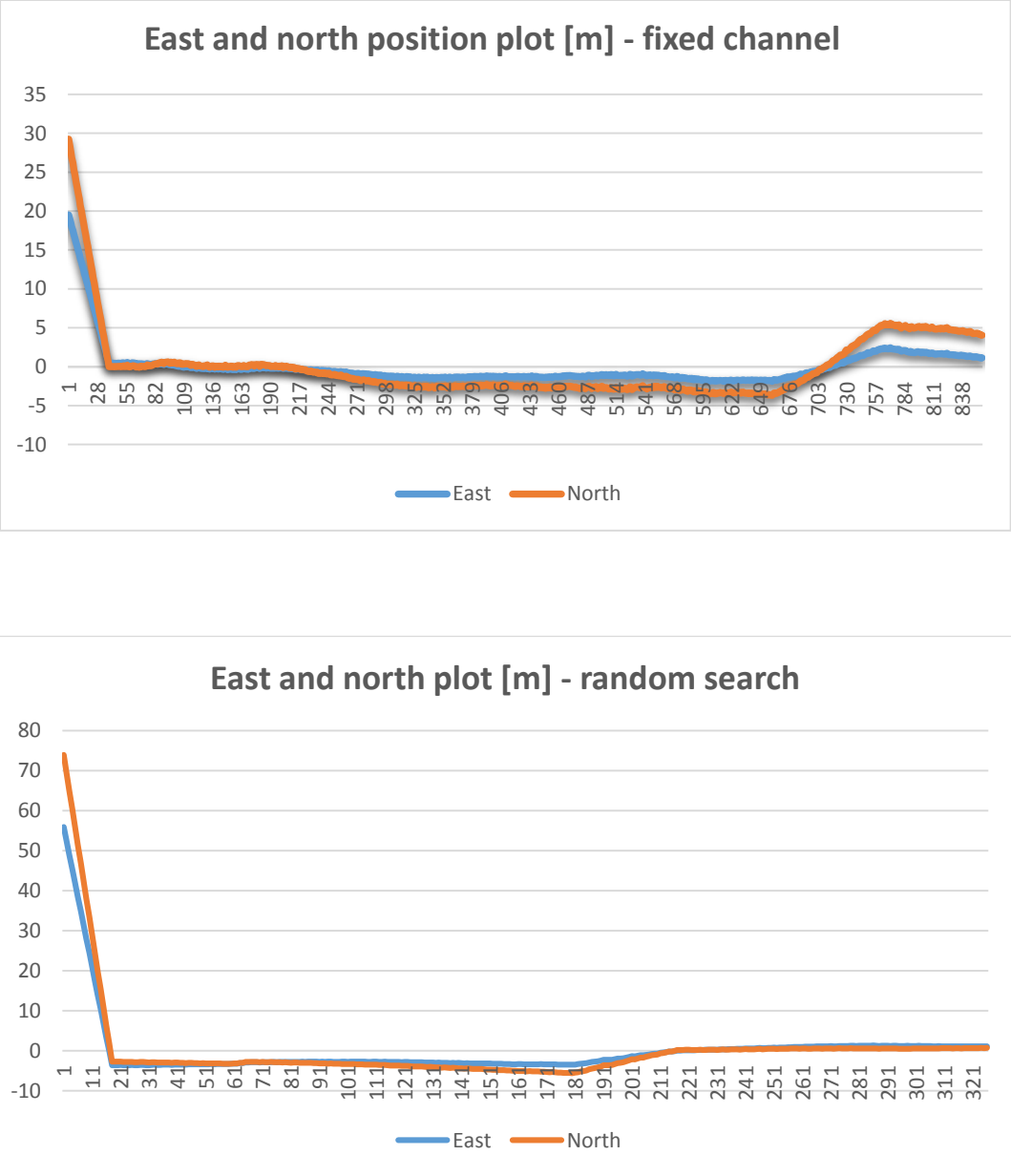

Figure 4-17 East and north plot (0 is their own average)

And the precision scatter plot is in Figure 4-18. Same as the weather effect experiment.

From the statistics table and scatter plot, it is clear that the random search method

somehow captures the signal which is different from the fixed channel search signal and change precision and accuracy of positioning. The detailed multipath effect on the pseudorange from the G4 is still unknown. But from the analysis above, it can be concluded that if SDR is inside the urban canyon. The way of avoiding or minimizing the multipath signal is to set the receiving channels to the satellites in the viewshed and ignore those satellites not in the viewshed.

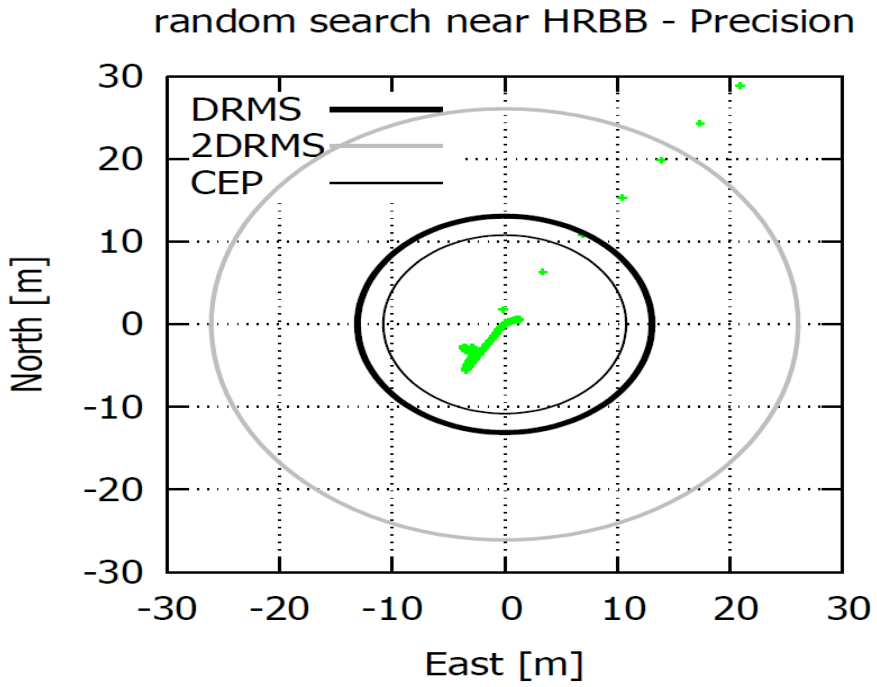

Figure 4-18 Precision plot near HRBB

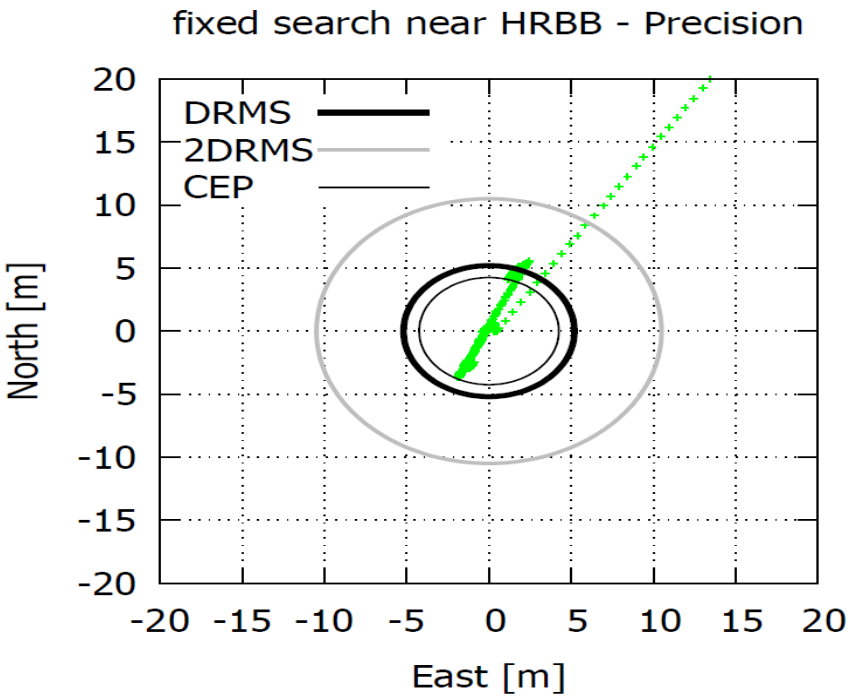

Figure 4-18 Continued

IV.7 Using hybrid GNSS system versus using single GNSS system

Introduction: With the development of GNSS system, the receivers nowadays have the ability to receive the signal from a hybrid GNSS system. For example, mobile phones using iOS or Android system can support both GPS and GLONASS navigation signal. In an urban canyon, as discussed before if the number of satellites which can directly send the signal to the receiver is lower than 4, the receiver can't locate itself in Chapter 1.

However, if the receiver can use satellites signal from multiple GNSS system, the number of satellites is greater than 4, the receiver can locate itself.

Aim: This experiment tends to find out how well the hybrid GNSS system comparing with single GNSS system by measuring the accuracy and precision of positioning.

Method: As the GNSS-SDR software can only support the reception of Galileo and GPS system, and there are only four Galileo satellites are in operational state, in which one of them is in repair. Our research group tried really hard to find out if there are any chances of doing real-time experiment, but we found out that is not the purpose of this experiment. So in this experiment, the data was already recorded and played back by SDR. The simulated results can still help to demonstrate the aim of the experiment. The recorded data can be played back using the option in GNSS-SDR software configuration file which can set the signal source to file signal source.

Results: Use the simulated data as showed in the table below, the hybrid system using both Galileo and GPS satellites has the worst performance comparing with single GNSS system.

	8 GPS	8 Galileo	4 GPS and 3 Galileo
Standard deviation East	1.1	1.37	1.89
Standard deviation North	1.7	1.27	2.42
CEP	1.7	1.56	2.57
2drms	2	3.7	6.2
Delta East (to actual)	-0.56	1.19	-1.81
Delta North (to actual)	1.32	1.92	3.6

Table 4-4 Hybrid system versus single GNSS system in [m]

But the accuracy and precision of using hybrid system is within the 5 meters which means that the hybrid system can't perform as the same as the single GNSS system, but Hybrid system can work well when the single GNSS system doesn't have enough satellites available as shown in Figure 4-19 on the accuracy and precision plot. One possible reason is perhaps the hybrid system only has 7 satellites comparing to single GPS or Galileo system which has 8 satellites.

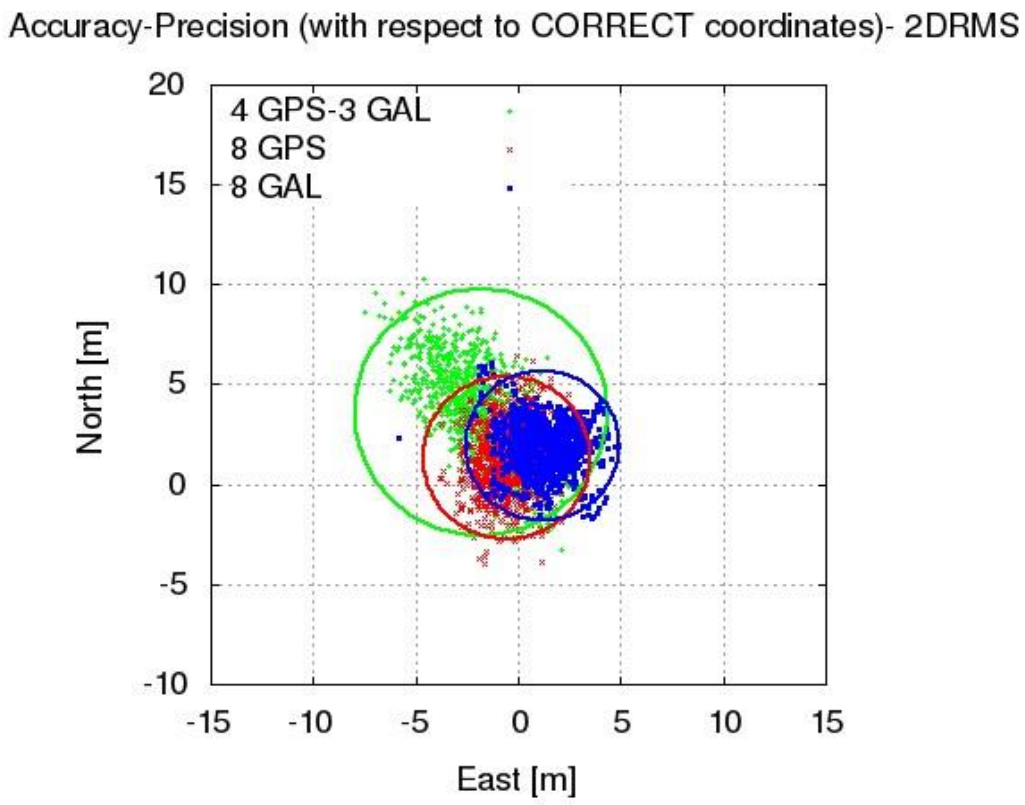

Figure 4-19 Accuracy and precision plot GNSS system [2]

If the hybrid system can have the exact number of the satellites, the result can be improved which can shrink the size of the green circle in Figure 4-19 and Table 4-4.

IV.8 Least square methods

Aim: GNSS-SDR software uses the least square method to calculate the position and speed, but the difference of using different averaging values is still unknown. This experiment is just testing the performance of using two separate least square averaging values.

Method: Place the SDR on the rooftop of HRBB with only the difference of least square averaging values. In the first run, the averaging value is 500, and in the second run. The value is 100.

Results: statistics table and the graphical plot of different averaging values are as the following.

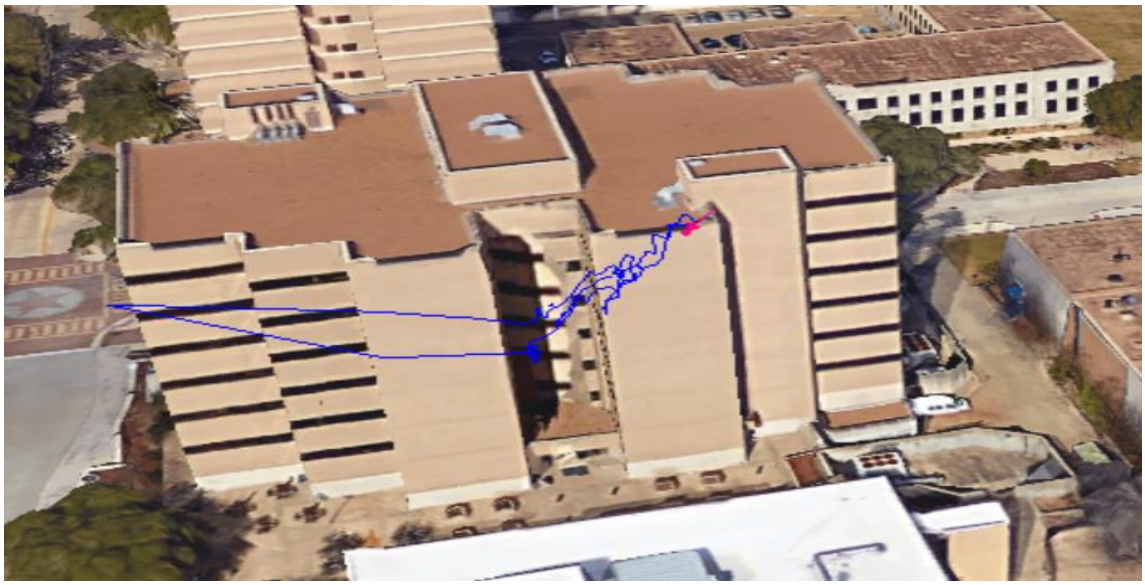

Figure 4-20 Google Earth Plot of different averaging number

In Figure 4-20, the red line is the averaging number 500 plot and blue line is the averaging 100 plot. The less the number of averaging, the more fluctuations of the location are.

Here is their east and north location plot, it is obtained using the same methodology the experiment of the effect of weather.

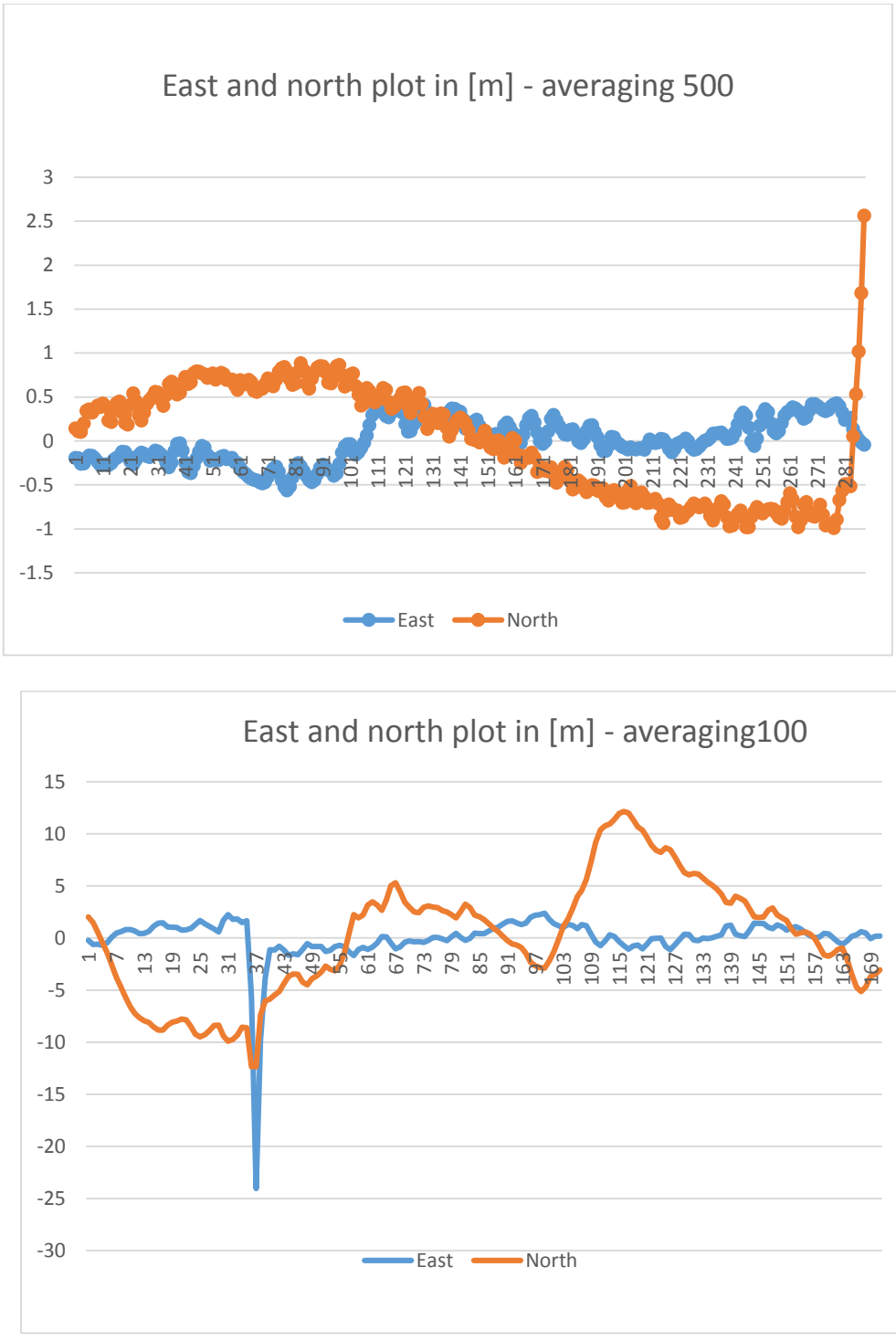

Figure 4-21 East and north plot least square (0 is their own average)

	Average 500	Average 100
Standard deviation East	0.24	2.27
Standard deviation North	0.64	5.7
CEP	0.52	4.7
2drms	1.36	12.26
Delta East (to actual)	36.3	35.92
Delta North (to actual)	-13.2	-23.56

Table 4- 5 Statistics analysis of different averaging

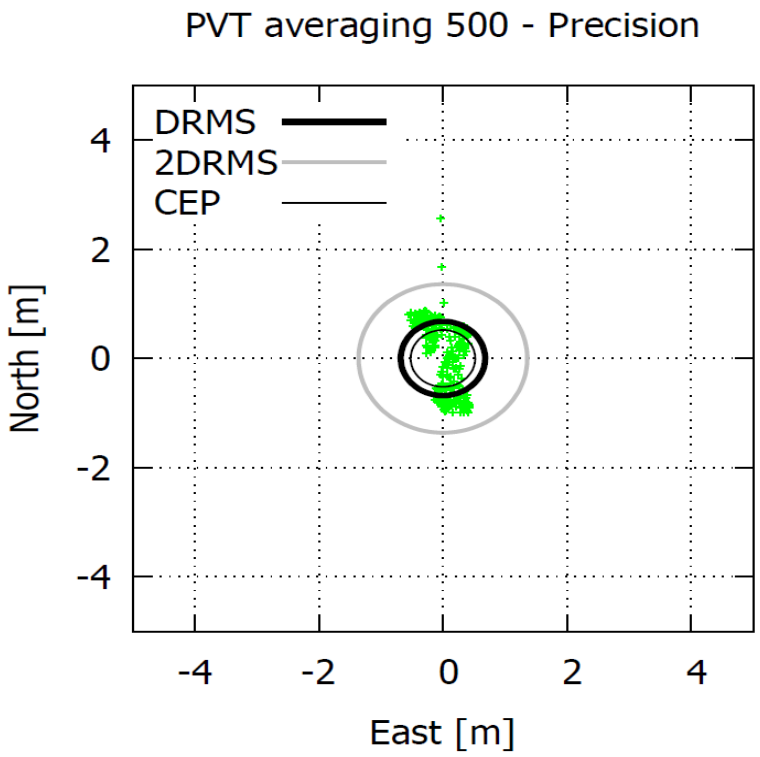

Figure 4-22 least square averaging precision plot

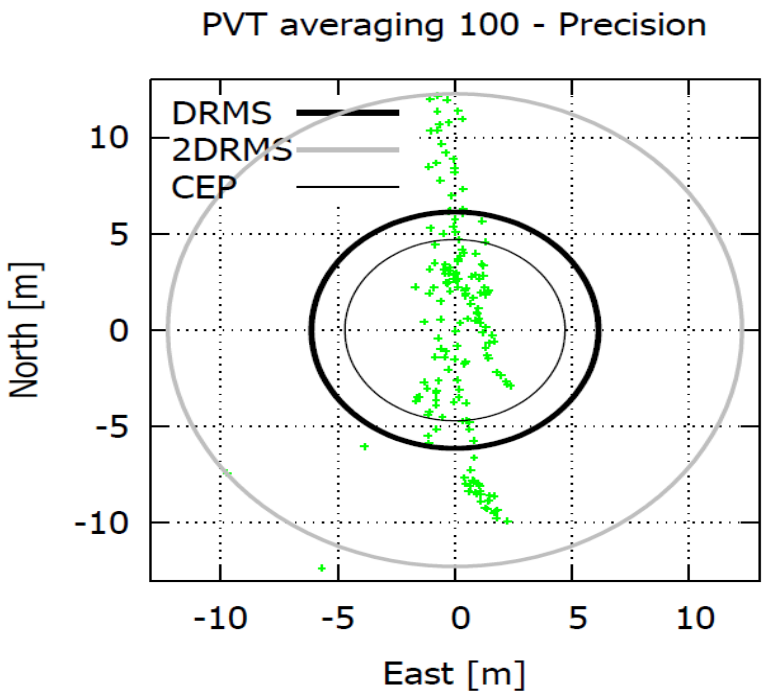

Figure 4-22 Continued

Using the same methodology in effect of weather experiment to analyze the GNSS data in Table 4-5. The EN plot and scatter plot are shown in Figure 4-21 as well as Figure 4-22. It can be observed that the higher of the averaging number of the algorithm the better the accuracy and precision of positioning is. The possible reason is the algorithm used in the software package is not that sophisticated which means the user can implement customer design of calculating the position.

IV.9 Using SDR as a moving receiver

Introduction: GPS navigation products can be seen every day in cars, and it measures the moving location and speed. If the SDR can only measure the static location, that would restrict the ability of the receiver to improve the algorithm to calculate the position and speed in real-time.

Aim: This experiment is trying to test the locating ability of the platform to see if whether or not the current least square algorithm is good enough for moving object test and whether the algorithm can be improved to conduct such experiment.

Method: The SDR is placed on the moving car. The antenna is attached to the top of the car. The route of the moving car was recorded as well as the calculated moving path of the receiver. Compare the two routes and find out if the algorithm of the receiver can be improved. The actual route is from Google Map.

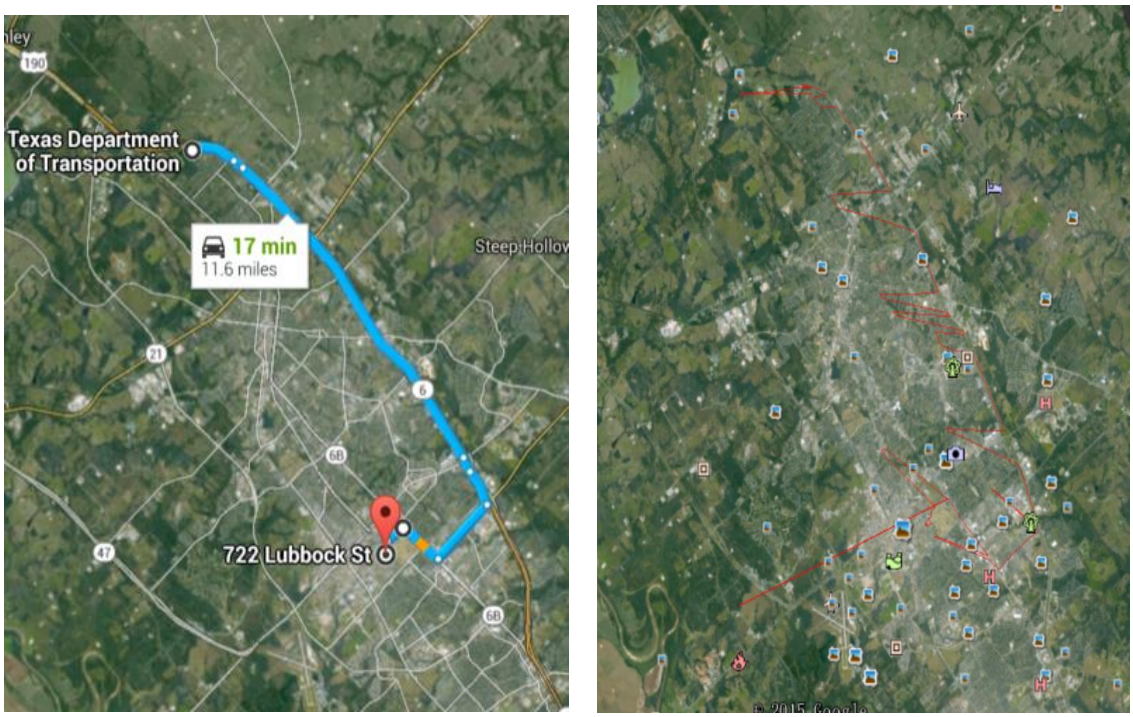

Figure 4-23 Actual route (left) VS measured route (right)

Results: Figure 4-21 is the comparison of the actual route of the car driving from CORS in Bryan to Texas A&M campus with the route measured using the SDR.

In Figure 4-21, on the left is the actual route, on the right is the measured route from the software.

From the comparison of the graph it can be observed that SDR in the moving car may not give a good measurement of the actual route as the least square algorithm uses the method which averages the raw location points and merges to a more precise location point which can be observed on the measured route plot as the spikes of the red line. The

ambiguous points swinging from the actual route are possibly those pseudorange drifting from the actual ones in pseudorange comparison experiment. Without these spikes, the route is similar to the actual one. We believe the commercialized navigation GPS such as Garmin and TomTom can use a more sophisticated method such as Kalman filter to eliminate the effect of the inaccuracy of the pseudorange from initialization or possibly clock drifting.

CHAPTER V

CONCLUSIONS AND FUTURE WORK

V.1 Conclusions

In this thesis, we built a portable GNSS research platform which is feasible to carry out experiments to verify the factors which can contribute to the accuracy and precision of SDR locating ability. The open source software GNSS-SDR provided us with the reconfigurable architecture which can be modified to track the specific GNSS satellite signal and use the hybrid system to validate those key factors in SDR positioning. For example, the effect of troposphere, ionosphere and PVT algorithm.

By conducting various experiments at different locations, we can find out that the results obtained from real-time experiment can demonstrate some critical issues in GNSS signal reception, for instance, the multipath problem and user clock problems. The experimental results are not only providing us with how crucial for a particular location the signal reception condition is, but also guiding us to develop the new algorithm and new methodology for minimizing the effect of those factors which can cause errors in positioning. From the experimental data analysis, it can be verified that we can change the configuration of the SDR and develop new methodology to minimize the errors contributing to the positioning and those experimental data can be reused and played back for the future GNSS research needs. The software itself can create the RINEX file,

NEMA file and PVT file which can be post-processed and evaluated in various GNSS software to save future research and debugging time.

V.2 Future work

The SDR itself still has some issues with the user clock which can sometimes make the experiment results suspicious. In the future, the atomic clock can be attached to the USRP to minimize the effect of the user clock. The software uses the least square method to calculate the position, the results gained in real-time can be linear not random, we have to develop our own more sophisticated algorithm to calculate. Last but not least, although the data can be post-processed using DGPS and corrections, it is desirable that the software itself can obtain the information of the GNSS signals coming through 3G or LTE network.

REFERENCES

[1] Sullivan, Mark. "A Brief History of GPS." *TechHive*. TechHive, 9 Aug. 2012. Web. 24 May 2015. <http://www.techhive.com/article/2000276/a-brief-history-of-gps.html>.

[2] Arribas, Javier. *GNSS SDR Array-based Acquisition: Theory and Implementation*. LAP LAMBERT Academic Publishing, 2013.

[3] Branzanti, Mara, Javier Arribas, Carles Fernandez-Prades, and Paul Closas. "Fastening GPS and Galileo Tight with a Software Receiver," *Proceedings of the ION GNSS+*, Tampa, FL, (2014): 1383 - 1395

[4] "USRP™ N200/n210 Networked Series." *Ettus Research*. Ettus Research, n.d. Web. 09 May 2015. <http://www.ettus.com/content/files/07495_Ettus_N200-210_DS_Flyer_HR_1.pdf>.

[5] "Choosing a GNSS Simulator?" *Spirent*. Spirent, n.d. Web. 09 May 2015. <http://www.spirent.com/~/media/eBooks/Positioning/Choosing_a_GNSS_simulator_eBook.pdf>.

[6] Guo, Ningyan, Staffan Backén, and Dennis Akos. "Building a Wide-Band Multi-Constellation Receiver: The Universal Software Radio Peripheral as RF Front-End." *GPS World* 24.3 (2013): 36-42.

[7] *National Geodetic Survey - CORS Team*. Digital image. *NOAA*. NOAA, n.d. Web. 16 June 2015. <http://www.ngs.noaa.gov/cgi-cors/corsage_2.prl>.

[8] Janssens, Johan, and Michiel Steyaert. "Receiver Architecture and Specifications." *CMOS Cellular Receiver Front-Ends: From Specification to Realization* (2002): 21-48.

[9] Tsui, James Bao-Yen. *Fundamentals of global positioning system receivers*. Wiley-Interscience, 2000.

[10] Parkinson, Bradford W. *Progress in Astronautics and Aeronautics: Global Positioning System: Theory and Applications*. Vol. 2. Aiaa, 1996.

[11] Dana, Peter H. "Global Positioning System Overview." *Global Positioning System Overview*. University of Colorado - Boulder, 2 May 2000. Web. 09 June 2015. <http://www.colorado.edu/geography/gcraft/notes/gps/gps.html>.

[12] Kim, Nam-Tae. "Ultra-wideband bias-tee design using distributed network synthesis." *IEICE Electronics Express* 10.15 (2013): 20130472-20130472.

[13] *Ettus.com Installing the Ettus Research GPSDO Kit for USRPTM N200 Series & E100 Series* (n.d.): n. pag. *Ettus Research*. Ettus Research. Web. 16 Mar. 2015. <www.ettus.com>.

[14] "Trimble GPS Tutorial - Error Correction." *Trimble*. Trimble, n.d. Web. 09 June 2015. <http://www.trimble.com/gps_tutorial/howgps-error.aspx>.

[15] Cui, Youjing, and Ge Shuzhi. "Autonomous vehicle positioning with GPS in urban canyon environments." *Robotics and Automation, IEEE Transactions on*19.1 (2003): 15-25.

[16] Kumar, Muthukumar. "GNSS Reflectometry: Making Use of Multipath for Altimeter Measurements! - Geoawesomeness." *Geoawesomeness*. Geoawesomeness, 29 Jan. 2014. Web. 24 May 2015. <http://geoawesomeness.com/gnss-reflectometry-making-use-multipath-altimeter-measurements/>.

[17] Irsigler, Markus, and Eissfeller Bernd. "Comparison of Multipath Mitigation Techniques with Consideration of Future Signal Structures," *Proceedings of the 16th*

International Technical Meeting of the Satellite Division of The Institute of Navigation (ION GPS/GNSS 2003), Portland, OR, (2003): 2584-2592.

[18] "Skyplot of Satellites." *Skyplot of Satellites*. Warnell School of Forestry and Natural Resources, n.d. Web. 24 Apr. 2015. <http://gps.sref.info/course/8e.html>.

[19] Groves, Paul D. "Shadow matching: A new GNSS positioning technique for urban canyons." *Journal of Navigation* 64.03 (2011): 417-430.

[20] "Google Summer of Code 2013 Ideas List." *Google Summer of Code 2013 Ideas List*. N.p., n.d. Web. 18 June 2015. <http://gnss-sdr.org/documentation/google-summer-code-2013-ideas-list?&session-id=1023d086a0e95a4e1f16451eaa57c138>.

[21] August, Peter, Joanne Michaud, Charles Labash, and Christopher Smith. "GPS for environmental applications: accuracy and precision of locational data." *Photogrammetric Engineering and Remote Sensing* 60, no. 1 (1994): 41-45.

[22] Huang, Lu, Wan-Rong Zhang, Hong-Yun Xie, Jia Li, Wei Zhang, Yang Wang, Pei Shen, Jun-Ning Gan, Yi-Wen Huang, and Ning Hu. "A low power SiGe HBT LNA utilizing serial inductance for wideband matching." In *Solid-State and Integrated-Circuit Technology, 2008. ICSICT 2008. 9th International Conference on*, IEEE, (2008): 1500-1503

[23] "Comparative Features List." *USRP Hardware Driver and USRP Manual: USRP2 and N2x0 Series*. N.p., n.d. Web. 18 June 2015. <http://files.ettus.com/manual/page_usrp2.html>.

[24] Frankel, Joe. *The Global Positioning System - GPS Technologies and Their Accuracies*. Atlanta: Georgia Institute of Technology, 10 Feb. 2003. PPT.

[25] Meguro, Jun-ichi, Taishi Murata, Jun-ichi Takiguchi, Yoshiharu Amano, and Takumi Hashizume. "GPS multipath mitigation for urban area using omnidirectional infrared camera." *Intelligent Transportation Systems, IEEE Transactions on* 10, no. 1 (2009): 22-30.